Research Report 2015-5
Civil & Natural Resources Engineering

UNIVERSITY OF CANTERBURY
Te Whare Wānanga o Waitaha
CHRISTCHURCH NEW ZEALAND

Horizontal Infrastructure Performance and Application of the Liquefaction Resistance Index Methodology in Christchurch City through the 2010-2011 Canterbury Earthquake Sequence

Misko Cubrinovski
Matthew Hughes
Brendon Bradley
John Noonan
Steve McNeill
Geoff English
Irmana Garcia Sampedro

ISSN 1172-9511

UC ENGINEERING

September 2015

Horizontal Infrastructure Performance and Application of the Liquefaction Resistance Index Methodology in Christchurch City through the 2010-2011 Canterbury Earthquake Sequence

Misko Cubrinovski[1], Matthew Hughes[1,2], Brendon Bradley[1],

John Noonan[3], Steve McNeill[3], Geoff English[3],

Irmana Garcia Sampedro[4]

[1] Department of Civil and Natural Resources Engineering, University of Canterbury

[2] Department of Geological Sciences, University of Canterbury

[3] Christchurch City Council

[4] Stronger Christchurch Infrastructure Rebuild Team

University of Canterbury

September 2015

Summary

This is the third and final report from the research study performed within the NHRP Research Project "Impacts of soil liquefaction on land, buildings and buried pipe networks: geotechnical evaluation and design, Task 3: Seismic assessment and design of pipe networks in liquefiable soils". The work presented herein is a continuation of the comprehensive study on the impacts of Christchurch earthquakes on the buried pipe networks presented in two reports (Cubrinovski et al., 2011; Cubrinovski et al., 2014) and several journal and conference publications. It is important to consider this report not in isolation, but rather as an extension and continuation of the previous two reports. For this reason, very limited coverage is presented herein on issues and details discussed in the preceding reports.

The main objective of this report is to present an overview of application of the Liquefaction Resistance Index developed by Cubrinovski et al. (2011), and to demonstrate its usefulness in quantifying actual earthquake observations and summarise them in the form of liquefaction zoning (hazard) map, and for quickly developing preliminary liquefaction zoning for the needs of Christchurch City Council (CCC) and their immediate decision-making before a more robust zoning/analyses based on high-quality geotechnical data could be completed. Also presented here are relationships between LRI zones and performance of critical horizontal infrastructure networks: potable water, waste water and roads.

For the potable water network there is a clear trend of increasing rate of repairs with decreasing liquefaction resistance of soils: (a) Highest repair rates are seen for LRI Zone 0 which has the lowest liquefaction resistance; (b) the repair rates decrease gradually with increasing LRI Zone number, (c) the lowest repair rates are seen for LRI Zone 4. The rate of repairs in LRI Zone 0 is about 25 times greater than that in LRI Zone 4. This is consistent with the expectation that liquefaction-induced ground deformation is a governing factor in the damage to buried pipes, and hence presents an independent validation of the LRI concept and its applicability. For the waste water network, there is a clear trend in the repairs rate as a function of the LRI Zone number or liquefaction resistance of soils. LRI Zone 0 is characterized by about 6 repairs per kilometre, which is 10 times higher than the repairs rate of LRI Zone 3 and nearly 200 times the repairs rate of LRI Zone 4. For the road network, there is in general a consistent trend of increase in rates of damage features with a decrease in the liquefaction resistance of soils (or decrease in the LRI Zone number). Our analysis results derived in this study can be used to develop a predictive tool for evaluating the performance of potable and waste water pipes of similar characteristics in future earthquakes affecting urban areas of New Zealand.

Closed Circuit Television structural damage observations have been conducted for 53% of Christchurch City's waste water network (~20,000 pipes), comprising a voluminous and detailed record of earthquake impacts. Ongoing research using these data involves establishing relationships between structural damage and seismic and ground deformation information, including the LRI. A particular focus of research is influence of earthquakes on gravity pipe lifetimes, information on which will assist asset owners across New Zealand in managing long-term asset resilience and appropriate levels of service.

Table of Contents

List of Figures

List of Tables

List of Acronyms

AC	Asbestos Cement
CBD	Central Business District
CCC	Christchurch City Council
CCL	City Care Limited
CCTV	Closed-Circuit Television
CERA	Canterbury Earthquake Recovery Authority
CES	Canterbury Earthquake Sequence
CI	Cast Iron
CLS	Concrete-Lined Steel
CONC	Concrete
DI	Ductile Iron
EW	Earthenware
FH	Fulton Hogan
GI	Galvanised Iron
GIS	Geographic Information System(s)
GPS	Global Positioning System
HDPE	High-Density Polyethylene
LRI	Liquefaction Resistance Index
MDPE80	Medium-Density Polyethylene 80
MPVC	Modified Polyvinyl Chloride
PDA Tool	Pipe Damage Assessment Tool
PVC	Polyvinyl Chloride
RCRR	Reinforced Concrete Rubber-Ring jointed
S	Steel
SCIRT	Stronger Christchurch Infrastructure Rebuild Team
UC	University of Canterbury

1.0 Introduction

This is the third and final report from the research study performed within the NHRP Research Project "Impacts of soil liquefaction on land, buildings and buried pipe networks: geotechnical evaluation and design, Task 3: Seismic assessment and design of pipe networks in liquefiable soils". The work presented herein is a continuation of the comprehensive study on the impacts of Christchurch earthquakes on the buried pipe networks presented in two reports (Cubrinovski et al., 2011; Cubrinovski et al., 2014) and several journal and conference publications. It is important to consider this report not in isolation, but rather as an extension and continuation of the previous two reports. For this reason, very limited coverage is presented herein on issues and details discussed in the preceding reports.

The main objective of this report is to present an overview of application of the Liquefaction Resistance Index developed by Cubrinovski et al. (2011), and to demonstrate its usefulness in quantifying actual earthquake observations and summarise them in the form of liquefaction zoning (hazard) map, and for quickly developing preliminary liquefaction zoning for the needs of Christchurch City Council (CCC) and their immediate decision-making before a more robust zoning/analyses based on high-quality geotechnical data could be completed. Also presented here are relationships between LRI zones and performance of critical horizontal infrastructure networks: potable water, waste water and roads. These relationships demonstrate the usefulness of the LRI for interpreting infrastructure performance through combinations of seismic demand and liquefaction resistance.

We also present a general overview of waste water assessments undertaken within the Stronger Christchurch Infrastructure Rebuild Team (SCIRT), and outline current and future research directions for this system.

2.0 The Canterbury Earthquake Sequence

Between September 2010 and December 2011, Christchurch, the second largest city of New Zealand (population: ~ 350,000; area: ~ 450 km^2), was damaged by a series of strong earthquakes: 4 Sept. 2010 (M_w = 7.1); 22 Feb. 2011 (M_w = 6.2, 185 fatalities); 13 June 2011 (two events: M_w = 5.3 at 1 p.m. and M_w = 6.0 at 2:20 p.m.) and 23 Dec. 2011 (two events: M_w = 5.8 at 1:58 p.m. and M_w = 5.9 at 3:18 p.m.) (Fig. 1; for detailed reviews of the geologic and seismic aspects of the CES, see Beavan et al., 2010, 2011, 2012a, 2012b; Duffy et al., 2013; Quigley et al., 2012; Bradley et al., 2014). The close proximity of causative faults to Christchurch generated strong ground motions (Bradley and Cubrinovski, 2011; Bradley, 2012) that caused extensive damage to residential and commercial properties (Cubrinovski et al., 2011a; Bray et al., 2014; Bech et al., 2014; Fleischman et al., 2014; Moon et al., 2014) and infrastructure lifelines, particularly potable water, waste water, and road networks (Cubrinovski, et al., 2011b; 2014a, 2014b, 2014c; O'Rourke et al., 2014). Much of the damage to the city's built environment was caused by widespread soil liquefaction that occurred predominantly in saturated, unconsolidated alluvial and marine fine sediments in east Christchurch, in the region of late Holocene coastal progradation. In susceptible soils with high water tables (e.g., suburbs adjacent to the Avon River), liquefaction was manifested at the ground surface in earthquakes as low as M_w 5.0 and PGAs as low as 0.08 g (Quigley et al., 2013). Less-susceptible soils

required higher shaking intensities for liquefaction initiation (Tonkin & Taylor, 2013; van Ballegooy et al., 2014b). Liquefaction caused significant ground deformations, ejection of groundwater and sediments on to the ground surface, and lateral spread around rivers (Cubrinovski et al., 2012; 2014c; Quigley et al., 2013; Green et al., 2014; van Ballegooy et al., 2014b). Liquefaction caused widespread and severe subsidence throughout eastern and central Christchurch as a result of lateral spreading, topographic re-levelling, volume loss due to water, sand and silt ejecta to the ground surface and post-liquefaction volumetric densification. In some areas, loadings from structures and preferential ejecta pathways through roads and buried infrastructure imparted distinct anthropogenic signatures on surface ejecta patterns, and subsidence across eastern Christchurch has exacerbated longstanding flooding issues and vulnerability to tsunami and sea-level rise impacts (Hughes et al., 2015).

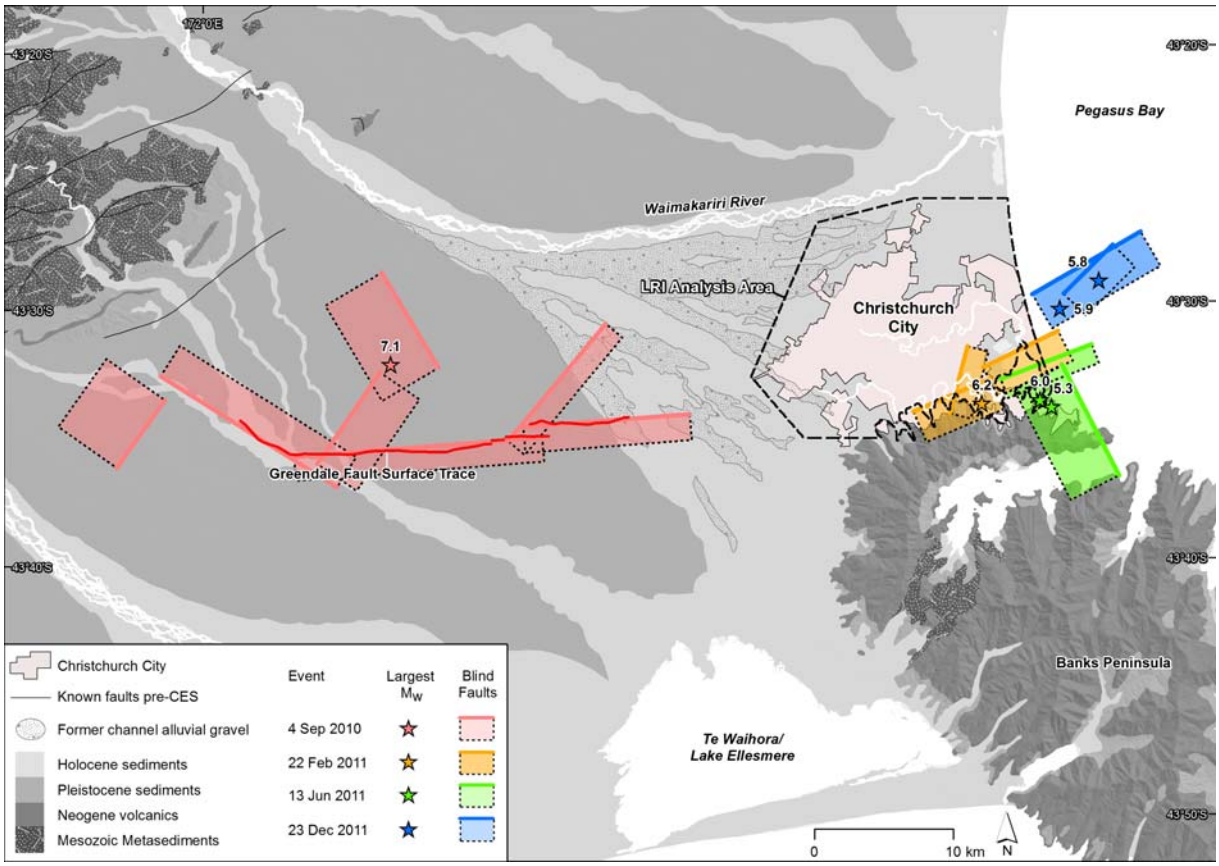

Figure 1. Geologic context of the CES, with major epicentres and blind fault locations shown. Also shown are the urban extent of Christchurch City, and the Liquefaction Resistance Index (LRI) analysis area addressed in this report.

3.0 Liquefaction Resistance Index concept

In the simplified procedure for liquefaction evaluation (e.g. Youd et al., 2001; Boulanger and Idriss, 2014) a factor of safety against triggering of liquefaction (in a free field level ground deposit), *FS*, is calculated as

$$FS = \frac{CRR_{7.5,100}}{CSR} MSF \times K_{\sigma} \quad (1)$$

where $CRR_{7.5,\ 100}$ is the Cyclic Resistance Ratio or liquefaction resistance while *CSR* is the Cyclic Stress Ratio which represents the earthquake load (seismic demand). The subscripts in $CRR_{7.5,\ 100}$ indicate that *CRR* is defined for a reference magnitude 7.5 earthquake (i.e. 15 significant cycles of shear stresses) and an effective overburden stress of 100 kPa. In cases when the earthquake magnitude is different than 7.5 and the effective overburden stress is different than 100 kPa the reference $CRR_{7.5,\ 100}$ value is modified using the Magnitude Scaling Factor (*MSF*) and K_σ correction factor respectively In essence, *CSR* accounts for the amplitude of the seismic load (using the peak ground acceleration as a measure for the amplitude shear stresses) while *MSF* accounts for the duration of shaking (or number of significant loading cycles) using the earthquake magnitude as a proxy for the shaking duration. According to Idriss and Boulanger (2008), the *MSF* is given by

$$MSF = 6.9 \times exp\left(-\frac{M_w}{4}\right) - 0.058 \leq 1.8 \tag{2}$$

where M_w is the moment magnitude of the earthquake. In the simplified triggering procedures it is often adopted to use K_σ = 1.0 for shallow depths with effective vertical stresses of $\sigma'_v \leq 100$ kPa. Hence, for shallow depths, Eq (1) can be reduced to

$$FS = \frac{CRR_{7.5}}{CSR} MSF \tag{3}$$

If $FS \leq 1.0$, then the available liquefaction resistance is smaller than (or equal to) the earthquake load (demand) and hence liquefaction will be triggered (will occur) for the adopted earthquake loading (*PGA* and M_w. The simplified method is used as a predictive tool to evaluate the liquefaction triggering at a given site for an assumed ground motion (Peak Ground Acceleration, *PGA*; Moment Magnitude, M_w) and estimated liquefaction resistance $CRR_{7.5}$ using empirical relationships based on penetration resistance or shear wave velocity.

Using this approach and Eq (3), the inverse problem could be solved to back-calculate the liquefaction resistance $CRR_{7.5}$ based on records of ground motions and observed liquefaction manifestation in an earthquake event. Provided that ground motions have been recorded by a relatively dense array of instruments, and liquefaction manifestation in the area/sites of the instruments has been well-documented for a given earthquake event, CSR, MSF and FS can be calculated/estimated as follows: *CSR* is calculated for each instrumented site using the recorded peak ground acceleration (*PGA*); *MSF* is computed (estimated) for the whole area using the earthquake magnitude (M_w) of the event; and, the factor of safety against liquefaction triggering *FS* is estimated based on the severity of the observed liquefaction manifestation at the site of interest. Note that empirical liquefaction triggering criteria were actually developed based on observed manifestation (or lack of it) of liquefaction on the ground surface in well-documented case histories, and hence the aforementioned approach in evaluating FS is consistent with the simplified liquefaction triggering procedure. Eventually, the liquefaction resistance or $CRR_{7.5}$ is back-calculated as:

$$CRR_{7.5} = \frac{CSR \cdot \overline{FS}}{MSF} = CSR_{7.5} \cdot \overline{FS} \tag{4}$$

Here $CSR_{7.5}$ is a function of *PGA* and M_w whereas $\overline{FS}$ is the estimated factor of safety as a function of the severity of liquefaction manifestation. This approach was adopted to first estimate $CRR_{7.5}$ and

then calculate a so-called Liquefaction Resistance Index (*LRI*), produce an *LRI* map and develop liquefaction zoning for Christchurch based on *LRI*, as described below.

There are a couple of advantages of this approach. First, it allows us to quantify actual earthquake observations and summarize them in the form of liquefaction zoning (hazard) map. Second, using this approach we could quickly develop preliminary liquefaction zoning for the needs of CCC and their immediate decision-making before a more robust zoning/analyses based on high-quality geotechnical data could be completed.

3.1 $CSR_{7.5(wt)}$ values from the Darfield and Christchurch earthquakes

$CSR_{7.5}$ is a function of the PGA on the ground surface, considered depth in the deposit and water table depth, i.e. $CSR_{7.5} = f[PGA, r_d(z), wt(z)]$. For shallow depths, at and above the water table, there are no effects of r_d and $wt(z)$ on *CSR*, and the cyclic stress ratio is effectively a function of *PGA* alone, i.e. $CSR(wt) = f[PGA]$, or in terms of the reference 7.5 magnitude, $CSR_{7.5}(wt) = f[PGA, MSF]$. Thus, using the geometric mean peak ground accelerations recorded at the strong motion stations within and in the vicinity of Christchurch during the Darfield and Christchurch earthquakes, cyclic stress ratio values at the depth of the water table $CSR_{7.5}(wt)$ were computed at the strong motion stations and then were interpolated across Christchurch using ordinary kriging interpolation.

For the Christchurch potable water system the pressurised pipe network is typically at shallow depths of about 0.5 m to 0.8 m, while the wastewater pipes are predominantly at depths from 2.0-3.5 m. Importantly, for most of the suburbs that experienced liquefaction in Christchurch, the water table was high, at about 1 m to 2.0 m from the ground surface (van Ballegooy et al., 2014). Hence, the $CSR_{7.5}(wt)$ values estimated as above accurately represent the seismic demand (earthquake loads) specific to liquefaction for depths corresponding to embedment depths of the potable water (PW) and waste water (WW) pipelines. For these reasons, the liquefaction zoning for pipe networks was focused on the shallow depths of the deposits corresponding to the depth of the water table (or slightly below) yielding the final form of the expression for the Cyclic Resistance Ratio:

$$CRR_{7.5(wt)} = \frac{CSR_{7.5(wt)} \cdot \overline{FS}}{MSF} = CSR_{7.5(wt)} \cdot \overline{FS} \qquad (5)$$

where $CRR_{7.5(wt)}$ is the cyclic resistance ratio corresponding to the water table depth or to the embedment depth of embedment PW and WW pipelines.

3.2 Estimated $\overline{FS}$ values based on liquefaction observations from the Darfield and Christchurch earthquakes

A key issue in the calculation of LRI maps is the assumption/evaluation of the factor of safety $\overline{FS}$. We have to assume/estimate the value of the factor of safety for both areas that did liquefy, and areas that did not liquefy during the earthquakes.

For the liquefied areas, the factor of safety was defined based on the severity of manifested liquefaction on the ground surface, as follows. Since triggering of liquefaction yields by definition *FS* = 1.0, traces of liquefaction, low to moderate liquefaction and moderate to severe liquefaction were given $\overline{FS}$ values of 0.9, 0.75 and 0.50 respectively. In other words, $\overline{FS}$ decreases with increased severity of liquefaction manifestation. An $\overline{FS}$ of 0.5 indicates that the available cyclic strength of the

soil was half of the seismic load induced by the earthquake. For cases of extreme or very severe effects of liquefaction, an $\overline{FS}$ value of 0.25 was adopted to depict very poor ground performance and extremely low liquefaction resistance of soils.

In non-liquefied areas, it was conservatively adopted that in areas where the water table was at 1m or 2m depth, the $\overline{FS}$ was 1.1 and 1.25, respectively, or slightly above the liquefaction triggering threshold of *FS* = 1.0. In other words, areas with high water table and seismic demand, but no manifestation of liquefaction, were assumed to have $CRR_{7.5(wt)}$ that is 10% to 25% above the corresponding CSR value. Then, for areas with larger depths to the water table, $\overline{FS}$ was increased with the water table depth since it is well known that a thick crust decreases the likelihood of occurrence and surface manifestation of liquefaction. Thus, $\overline{FS}$ = 1.5, 1.75 and 2.0 was adopted for areas with depth to water table of 3.0, 4.0 and 5.0m. Clearly, in the latter case the depth to the water table and embedment depths of the pipelines could be substantially different.

3.3 LRI (Liquefaction Resistance Index) Map for Christchurch

The above approach was applied to develop an LRI (Liquefaction Index resistance) map for Christchurch as described in Cubrinovski et al. (2011) (Figure 2). Well-documented liquefaction maps were used to quantify the severity of liquefaction and its distribution throughout Christchurch, and estimate $\overline{FS}$ while $CSR_{7.5(wt)}$ values and their spatial distribution were calculated using the magnitude and recorded PGAs for the Darfield and Christchurch earthquakes. Note that the UC liquefaction map (Cubrinovski and Taylor, 2011) was the principal map used in the evaluation of LRI, and that the T&T map was employed only in areas that were not covered by the UC map. By multiplying the $\overline{FS}$ values with the respective $CSR_{7.5(wt)}$ the LRI value was calculated and summarised in Figure 2 in the form of a Liquefaction Resistance Index map of Christchurch. Here orange, yellow, green and blue indicate Zones 1, 2, 3 and 4, with Zone 1 being the reference zone. The red zone covers predominantly the abandoned areas or the Residential Red Zone and is below the established threshold LRI value of 0.065. Note that the zone numbers also indicate the relative liquefaction resistance. Thus, for example, Zone 3 has three times the liquefaction strength of the lower bound value of Zone 1.

To further facilitate the use of the LRI map in preliminary design evaluations, Table 1 summarises the typical range of settlements, ground displacements and strains associated with each *LRI* zone. These are based on expert judgement and should be taken only as preliminary estimates with further updates to follow based on more robust interpretation and analysis. For the grey zone, there were no liquefaction observations/inspections, and therefore these areas are outside of the *LRI* zoning, and should be considered/evaluated separately.

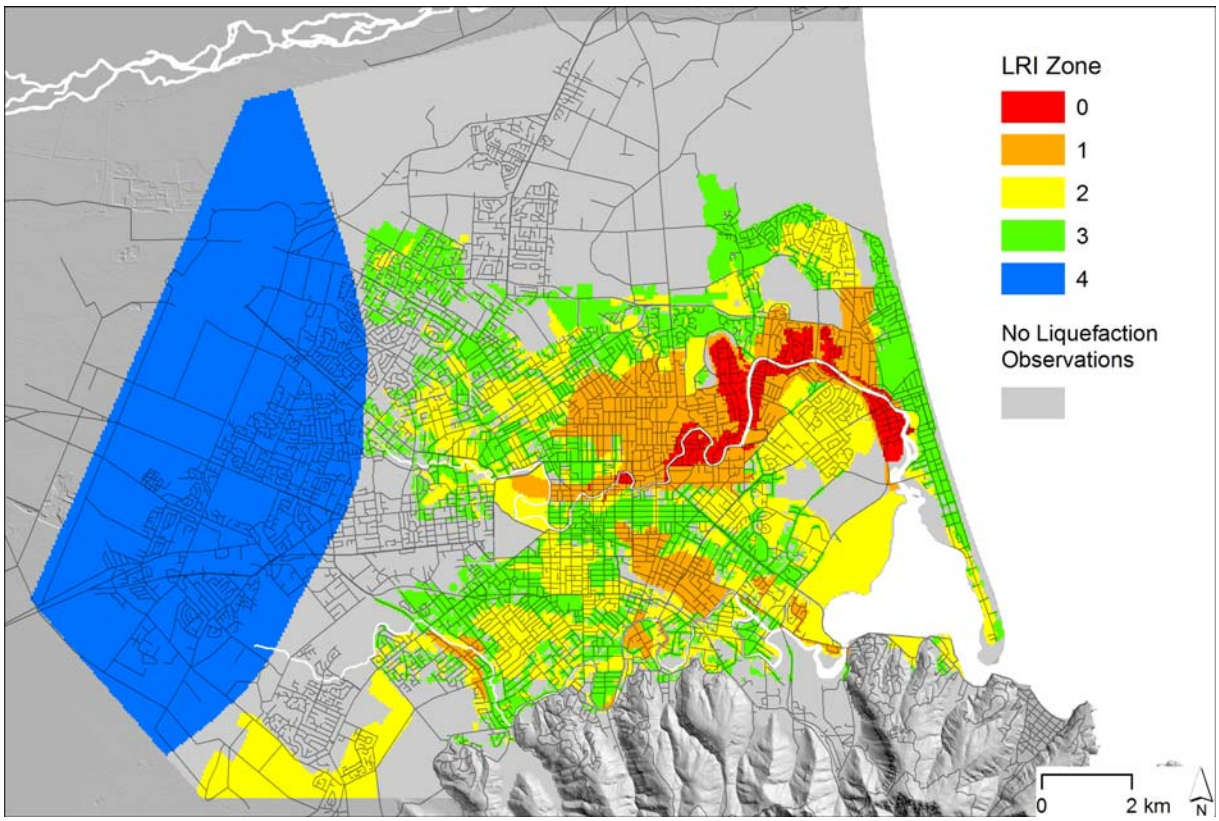

Figure 2. Liquefaction Resistance Index (Zoning) for Christchurch City. Associated ground deformations are shown in Table 1.

Table 1. LRI Zones and associated ground deformation (settlements, lateral displacements and strains).

LRI Zone	Equivalent CRR	Representative LRI (at water table)	Ground settlement (mm)	Lateral displacement (relative; transient) (mm)	Assumed ground strains and thickness of liquefied layer
0	< 0.065	-	> 500	> 400	ε_v > 5%, γ > 4%, H_L=5 – 10m
1	0.065 – 0.11	0.065	250 – 500	200 - 400	ε_v = 5%, γ = 4%, H_L=5 – 10m
2	0.11 – 0.16	0.13	50 – 250	40 - 200	ε_v = 3%, γ = 2%, H_L=4 – 8m
3	0.16 – 0.23	0.195	20 – 50	20 - 40	ε_v = 1%, γ = 1%, H_L=2 – 4m
4	> 0.23	0.26	< 20	< 20	γ < 0.5%, H_L=0m

- Design should accommodate the higher value of displacement/deformation

- ε_v = volumetric strain, γ = shear strain

4.0 $CSR_{7.5}$ through the Canterbury Earthquake Sequence

Details of the CSR calculations are provided below. At any given depth of a given deposit using (e.g. Idriss and Boulanger, 2008) *CSR* can be estimated using the following expression

$$CSR = 0.65 \frac{a_{max}}{g} \frac{\sigma_{vo}}{\sigma'_{vo}} r_d \tag{6}$$

where a_{max} is the PGA at the ground surface, σ_{vo} and σ'_{vo} are the total and effective overburden stress at depth (z), and r_d is a stress reduction factor as a function of depth. In the current analysis, i.e. at shallow depths of the ground water table (1 m to 3 m depths) this can be simplified to

$$CSR_{(wt)} = 0.65 \times PGA \tag{7}$$

where *PGA* is the recorded value at a particular recording station during the CES (Bradley and Hughes, 2012a;2012b). Note that σ_{vo}/σ'_{vo} = 1.0 at or above the ground water table, and r_d = 1.0 at shallow depths of less than 3-4 m. The *CSR* for an equivalent M_w = 7.5 is then given by

$$CSR_{7.5(wt)} = \frac{CSR_{(wt)}}{MSF} \tag{8}$$

with *MSF* given in Eq (2).

Moment magnitudes and *MSF* for each of the CES events considered in the below analysis are presented in Table 1. Maps of *PGA*, from Bradley and Hughes (2012a; 2012b), are presented for the major CES events across the LRI analysis area in Figure 3. Respective $CSR_{(wt)}$ values across the LRI analysis area calculated using Eq (5) are shown in Figure 4, and $CSR_{7.5(wt)}$ values across the LRI analysis area calculated using Eq (6), are shown in Figure 5. Figures 3(c), 4(c) and 5(c) include maximum *PGA*, $CSR_{(wt)}$ and $CSR_{7.5(wt)}$ values, respectively, from combined 4 September 2010 Darfield earthquake and 22 February 2011 Christchurch events.

Figure 6 summarises frequency distributions of $CSR_{7.5(wt)}$ across different LRI zones for the major CES events. Figure 6a shows that LRI Zones 2, 3 and 4 were subjected to higher demand in the Darfield event than LRI Zones 0 and 1 which suffered severe liquefaction and lateral spreading damage. This in turn indicates that the severe liquefaction in Zone 0 that occurred during this event was not due to the higher demand, but conversely it was due to the relatively low liquefaction resistance of the soils in this zone. Similarly, LRI Zone 2 has equal or higher seismic demand than LRI Zones 0 and 1 in the February 2011 event, again suggesting that the liquefaction resistance or $CRR_{7.5(wt)}$ was the key factor that contributed to the different severity of liquefaction that was predominantly observed in the respective LRI zones.

For the proper interpretation of the liquefaction manifestation maps and their derivations, such as the LRI map, it is important to understand that these maps provide a generic interpretation for a given area showing the predominant features of liquefaction manifestation or derived liquefaction resistance for the area. They do not have accuracy at a property basis and should not be used for such discrimination or interpretation.

Table 2. Epicentre locations, Mw and MSF values for major CES events. See Figure 1 for M_w epicentre locations.

Earthquake date and name	Latitude	Longitude	M_w	*MSF*
4 September 2010 Darfield earthquake	-43.538	172.164	7.1	1.08
22 February 2011 Christchurch I	-43.566	172.691	6.2	1.41
13 June 2011 II	-43.564	172.743	6.0	1.48
23 December 2011 II	-43.530	172.7428	5.9	1.52

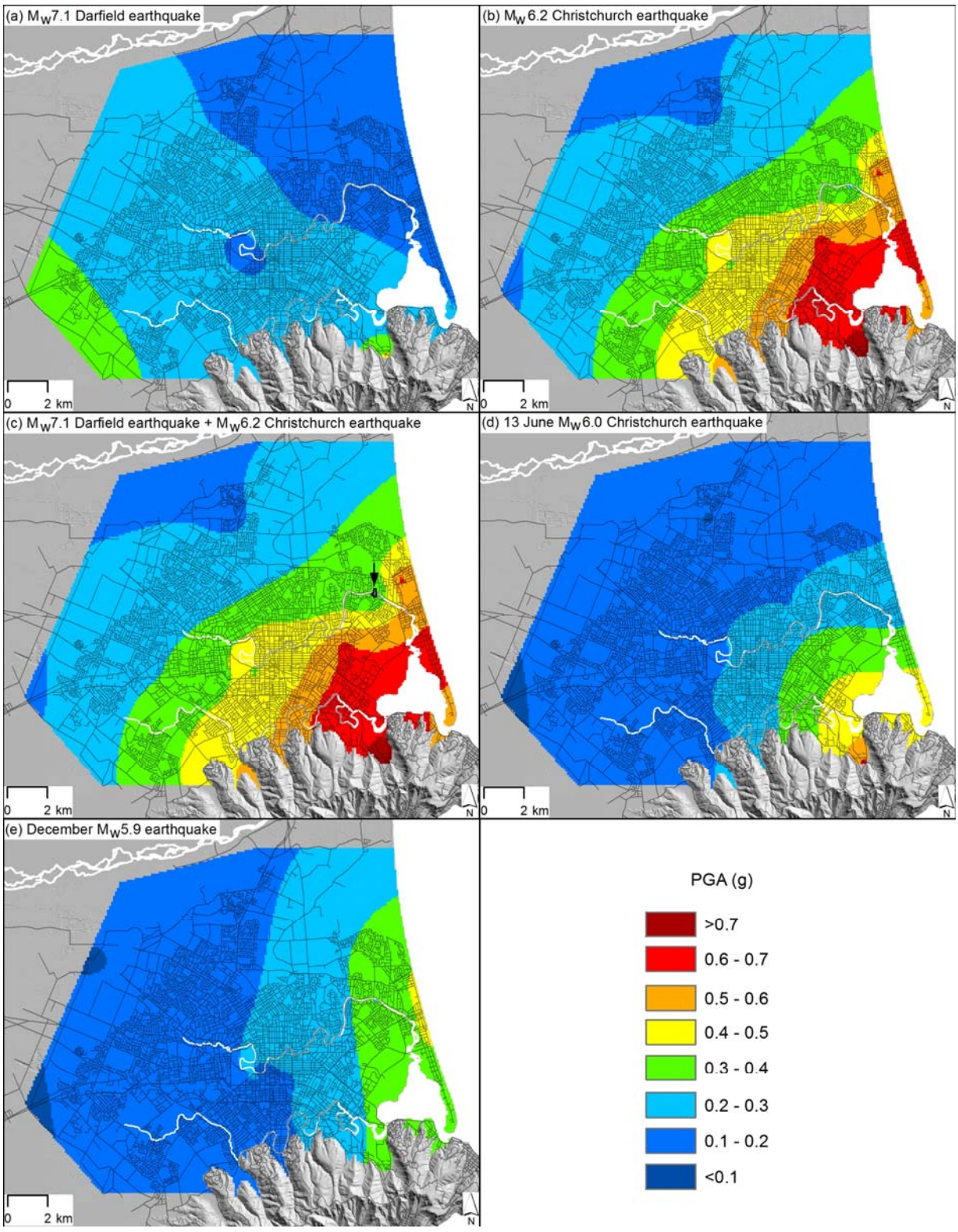

Figure 3. Peak Ground Acceleration (PGA) in units of gravity (g) for major CES events, within the LRI analysis area. PGA data are from Bradley and Hughes (2012a;2012b). Panel (c) shows combined highest PGA values from both the 4 September 2010 event (a) and 22 February 2011 event (b); the area where 4 September 2010 PGAs exceeded those of 22 February 2011 is indicated with a black arrow (<1% of analysis area).

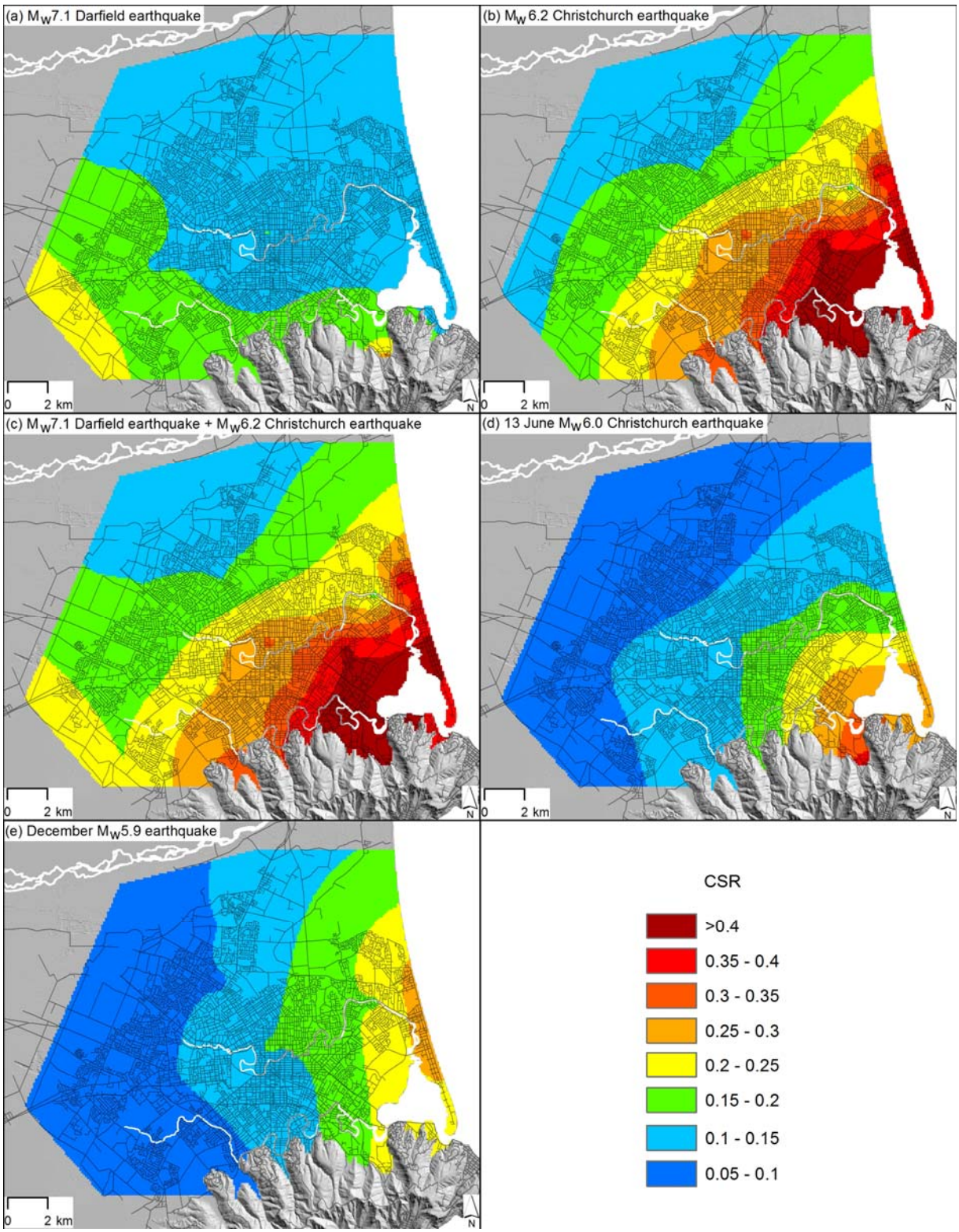

Figure 4. $CSR_{(wt)}$ within the LRI analysis area for major CES events, calculated from Equation 5.

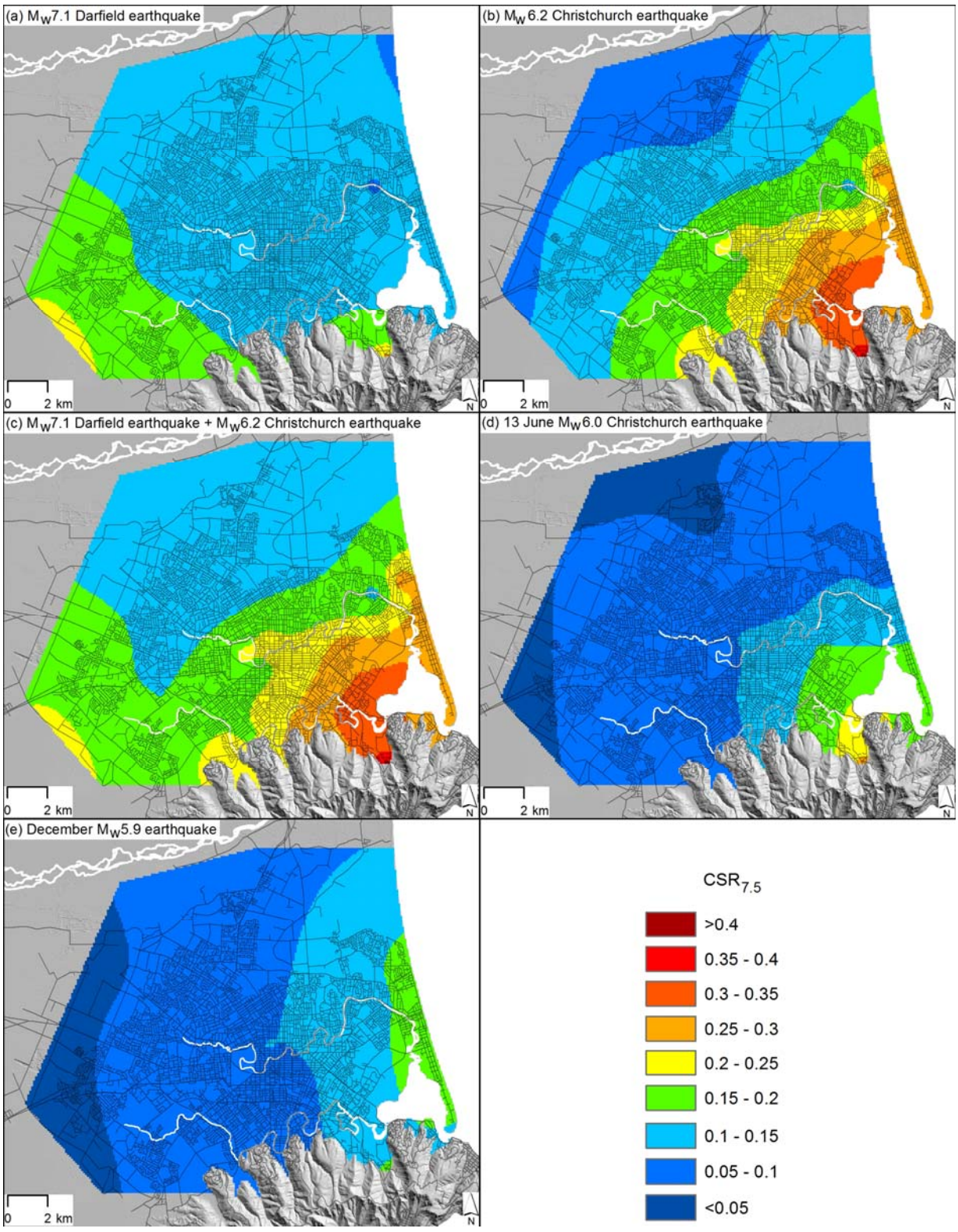

Figure 5. $CSR_{7.5(wt)}$ within the LRI analysis area for major CES events, calculated from Equation 6.

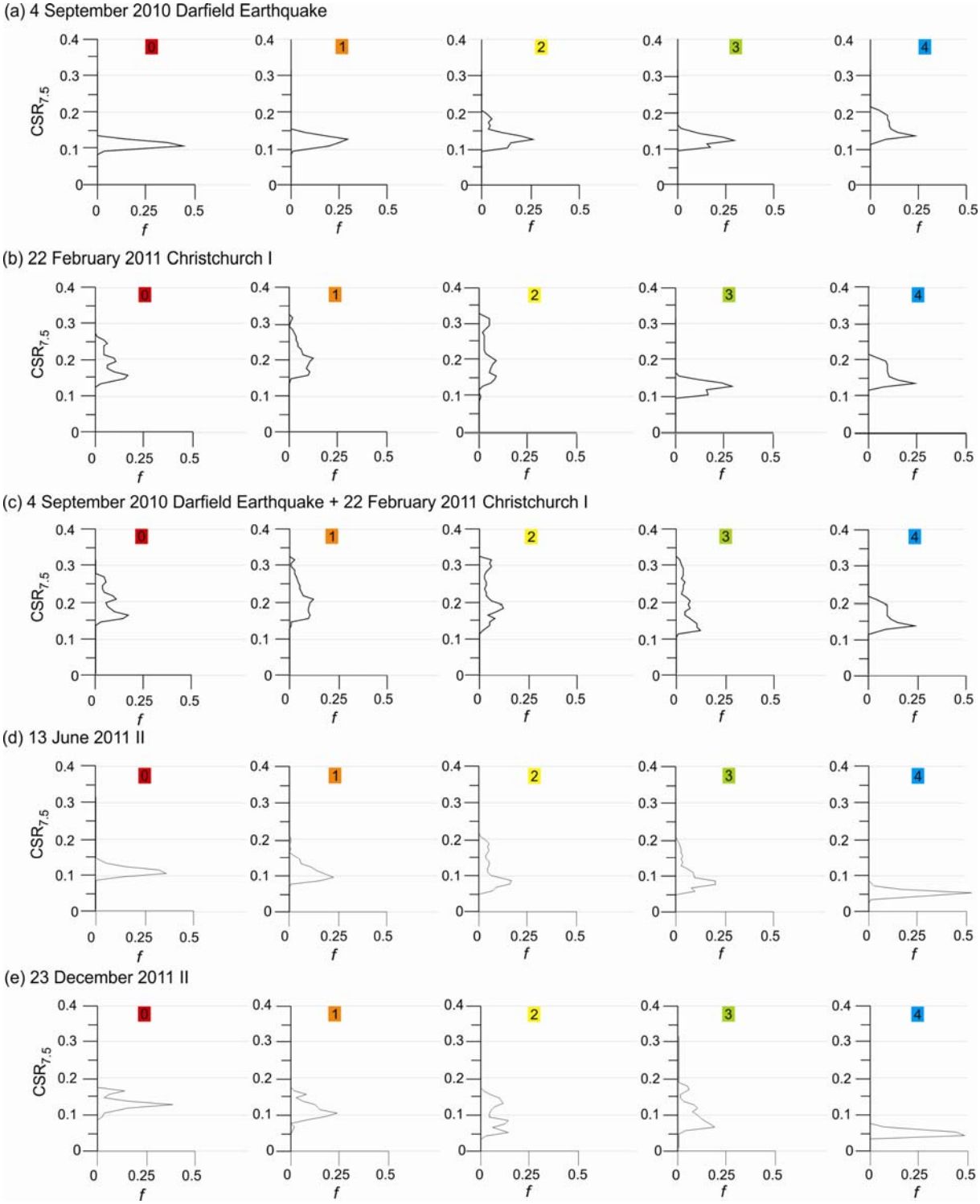

Figure 6. Frequency distributions (f) of $CSR_{7.5(wt)}$ across the spatial extents of LRI zones, for each major CES event.

5.0 Performance of Infrastructure Lifelines

Engineers of the Christchurch City Council (CCC) and SCIRT (Stronger Christchurch Infrastructure Rebuild Team) have compiled comprehensive evidence on the damage of the horizontal infrastructure either indirectly through activities focused on repair of faults and reinstatement of the lifelines or directly through inspections targeting identification of damage and its severity (e.g. CCTV and profilometer inspections of buried pipes). In our study, we have devoted a considerable effort and time to understand, organize and properly interpret these comprehensive datasets. The focus was first on the 'repairs data' since it was immediately available and relatively easy to apply in our engineering evaluations.

Potable water repair data are the same as used in Cubrinovski et al. (2014a), but repair rates are re-analysed here separately for the 22 February 2011, 13 June 2011 and 23 December 2011 events. Also presented here is an updated analysis of waste water performance based on repair locations following 22 February 2011. These waste water repairs are mainly emergency repairs in response to observations and complaints from the members of the public who notified the Christchurch City Council about obvious leaks or nuisance odours, and do not form a detailed picture of physical pipe damage. However their wide spatial extent across Christchurch City enables a preliminary understanding of the relative performance of waste water pipe types through the CES.

Also presented here are observations of damage to Christchurch City's road network. In the months after the 22 February 2011 events, the Christchurch City Council conducted widespread reconnaissance of the city's road network to ascertain damage to road pavement surfaces, kerbs and channels, and footpaths, with ~30,000 individual observations made. Here we present a subset of these data for road pavements (mapped cracks and potholes, uneven surfaces and ponding), and aggregated observations for kerbs and channels, and footpaths. For road pavement uneven surfaces, a more representative picture of damage is the percentage of road length in each LRI Zone affected, because a single observation could reflect damage along 1 m length or the entire length of a street.

Presented below are summary charts presenting performance in terms of number of repairs and repair rates (rates of repairs per kilometre length) across different LRI zones and pipe materials, and types of road surfaces. In these charts, repair rates (*RR*) are calculated as

$$RR = \frac{n}{L} \tag{9}$$

where *n* is the number of repairs performed on horizontal infrastructure or number of observed damage features, and *L* is the total length of horizontal infrastructure in a given LRI zone. Due to repair rates having a Poisson distribution the standard error (SE) of the repair rate is calculated as

$$SE = \frac{RR}{\sqrt{n}} \tag{10}$$

5.1 Potable Water

Figure 7 shows the distribution of the number of pipes (Fig. 7a) and length of pipes (Fig 7b) across the five LRI zones in Christchurch. Depending on the density of the network and size of each of the LRI

areas there is some variation in the number and lengths of potable water pipes, however, in each zone there are large number of pipes and a sufficient total length in the range from about 100 km to 700 km for a robust analysis. Figures 7c through 7e show the correlation between the rate of repairs (or repairs per kilometre) and LRI Zone for the February 2011, June 2011 and December 2011 earthquakes. They show a clear trend of increasing rate of repairs with decreasing liquefaction resistance of soils: (a) Highest repair rates are seen for LRI Zone 0 which has the lowest liquefaction resistance; (b) the repair rates decrease gradually with increasing LRI Zone number, (c) the lowest repair rates are seen for LRI Zone 4. The rate of repairs in LRI Zone 0 is about 25 times greater than that in LRI Zone 4. This outcome is fully consistent with the expectation that liquefaction-induced ground deformation is a governing factor in the damage to buried pipes, and hence presents an independent validation of the LRI concept and its applicability. There was insufficient data for the September 2010 event to be included in this analysis.

Figure 7 summarises the data for all pipe types. In order to understand the performance of different pipe types further analysis was conducted for the prevalent pipe materials for mains: Asbestos cement, Cast Iron, M-Polyvinyl chloride, Concrete-lined Steel, summarised in charts in Figure 8, and sub-mains: High-density Polyethylene, Medium-density Polyethylene, and Galvanised Iron pipes, summarised in Figure 9. In view of the fact that the February 2011 event was the most damaging and that records associated with the June 2011 and December 2011 earthquakes potential include damage caused by previous events and definitively include cumulative damage of the CES events, the repairs data associated with the February 2011 earthquakes is considered as the most reliable information (Figures 8c and 9c).

For the mains data, shown in Figure 8, the same trend is evident with the highest repair rates seen for the LRI Zone 0 and reduction in the rate of repairs with increase in the LRI Zone number. There is also a distinctive difference between the performance (repair rates) of brittle pipelines and ductile pipelines. For example, in LRI Zone 0, asbestos cement and cast iron have relatively high repair rates of about 9 per kilometre, concrete-lined steel and galvanized iron pipes have the highest repair rates of 12-19 per kilometre. On the other hand, the flexible pipelines (High-density Polyethylene, Medium-density Polyethylene, and M-Polyvinyl chloride) have much lower repair rates of 2-3 per kilometre. Importantly, the provided correlations provide basis for rigorous and detailed evaluation of the performance of different pipe materials or pipeline characteristics as a function of ground conditions and liquefaction resistance in particular. Note that LRI is directly related to a particular cyclic resistance or CRR as summarized in LRI, and hence, the analysis results derived in this study can be used to develop a predictive tool for evaluating the performance of potable water pipes of similar characteristics in future earthquakes affecting urban areas of New Zealand. It is important to note that other subtle but potentially important differences such as pipe diameters and connection details are subjects of further studies.

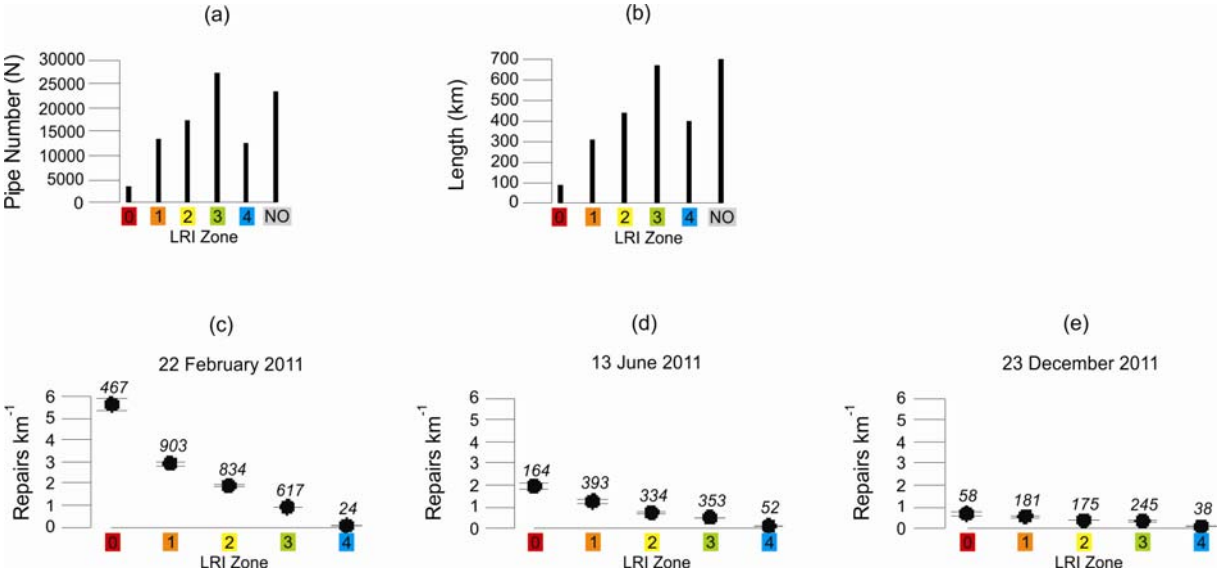

Figure 7. Potable water repairs for all major pipe types (Asbestos Cement, Cast Iron, M-Polyvinyl Chloride, Concrete-Lines Steel, High-Density Polyethylene, Medium-Density Polyethylene 80 and Galvanised Iron) in each Liquefaction Resistance Index (LRI) Zone. (a) Total number of pipes in each LRI zone, and areas of no liquefaction observations (NO). (b) Total pipe length (km) in each LRI zone, and areas of no liquefaction observations (NO). (c-e) Repair rates in each LRI zone and for the events of 22 February, 13 June and 23 December 2011, with standard errors indicated. Also shown are number of repairs (in *italics*) for each LRI zone.

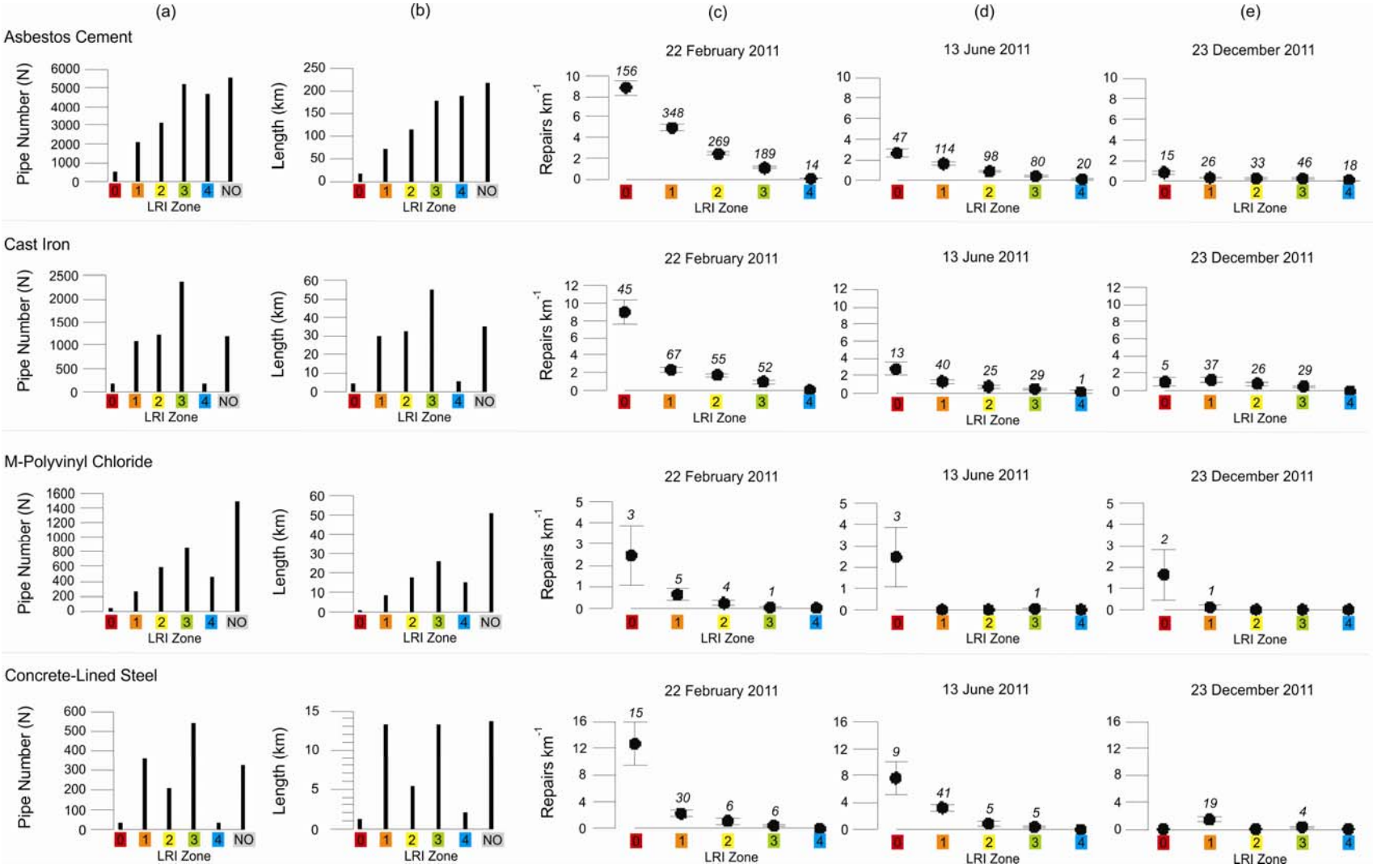

Figure 8. Potable water repairs for each Liquefaction Resistance Index (LRI) Zone and mains pipe materials. (a) Total number of pipes in each LRI zone, and areas of no liquefaction observations (NO). (b) Total pipe length (km) in each LRI zone, and areas of no liquefaction observations (NO). (c-e) Repair rates for each LRI zone and events of 22 February, 13 June and 23 December 2011, with standard errors indicated. Also shown are number of repairs (in *italics*) for each LRI zone.

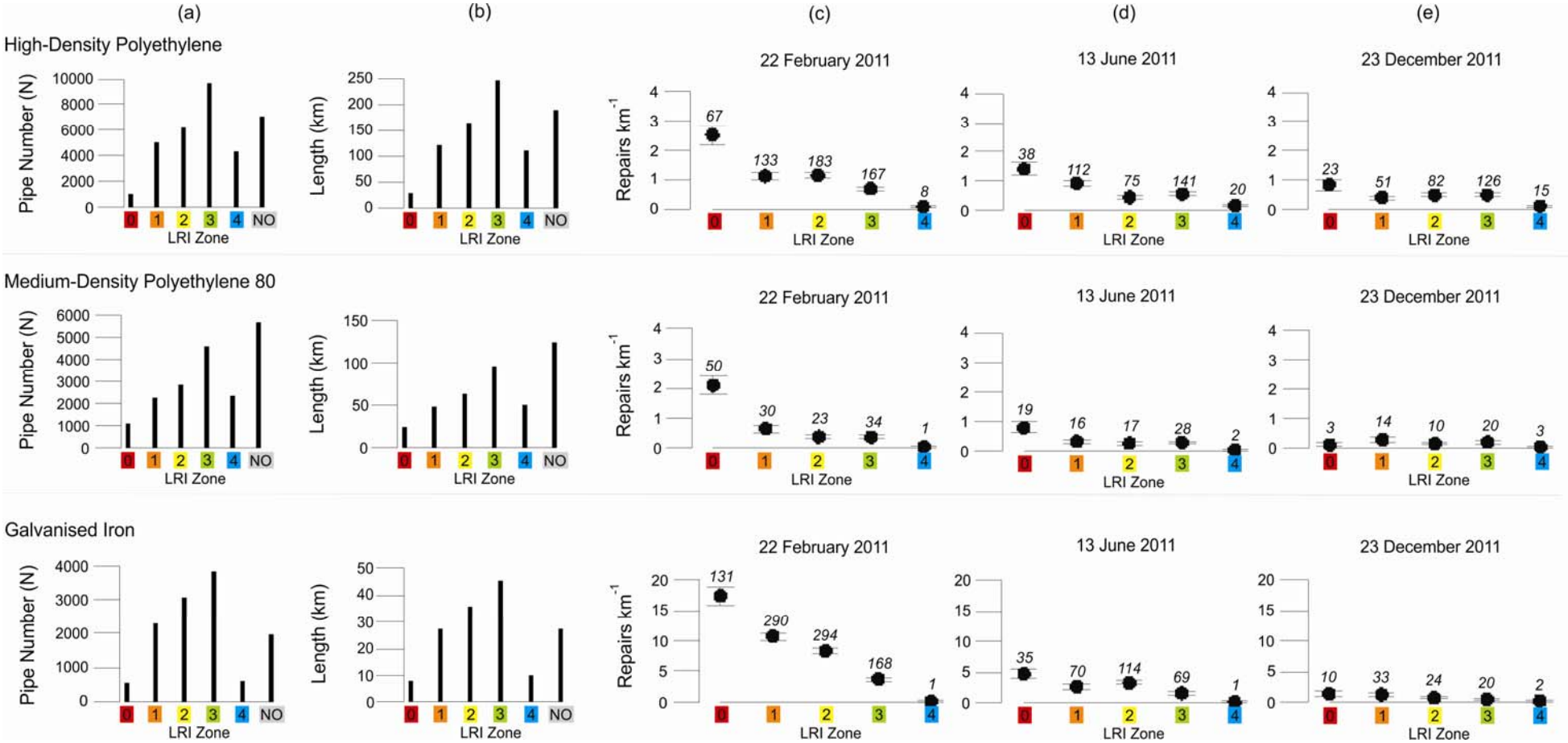

Figure 9. Potable water repairs for each Liquefaction Resistance Index (LRI) Zone and submains pipe materials. (a) Total number of pipes in each LRI zone, and areas of no liquefaction observations (NO). (b) Total pipe length (km) in each LRI zone, and areas of no liquefaction observations (NO). (c-e) Repair rates for each LRI zone and events of 22 February, 13 June and 23 December 2011, with standard errors indicated. Also shown are number of repairs (in *italics*) for each LRI zone.

5.2 Waste Water

An equivalent analysis for the waste water pipes is presented in this section and summarised in Figures 10 and 11. Here no distinction is made between individual CES events, although most repairs appear to be in response to 22 February 2011 and to a lesser extent 13 June 2011 and 23 December 2011. Again, there is a clear trend in the repairs rate as a function of the LRI Zone number or liquefaction resistance of soils. LRI Zone 0 is characterized by about 6 repairs per kilometre, which is 10 times higher than the repairs rate of LRI Zone 3 and nearly 200 times the repairs rate of LRI Zone 4.

Consistent with the potable water pipes performance, more ductile materials and flexible pipelines of the waste water network, such as PVC pipes, performed reasonably well showing low and tolerable repair rates across LRI Zones 1 to 4. Conversely, brittle material pipes and less flexible waste water pipelines of earthenware, asbestos cement, concrete, and reinforced concrete rubber-ring jointed show much higher repair rates particularly in zones of lower liquefaction resistance (LRI Zones 0, 1 and 2). Note that some of the results for PVC and polyethylene pipes are based on small number of pipes and hence the associated errors are significant and the evidence is inconclusive due to these limitations of the subset.

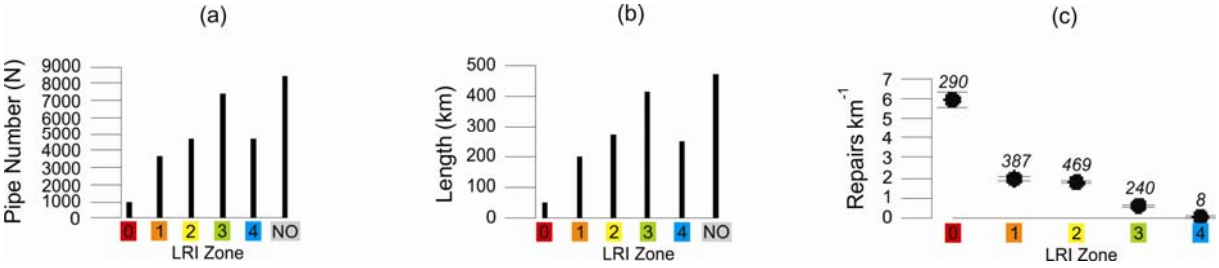

Figure 10. Waste water repairs for all major pipe types (Asbestos Cement, Cast Iron, M-Polyvinyl Chloride, Concrete-Lines Steel, High-Density Polyethylene, Medium-Density Polyethylene 80 and Galvanised Iron) in each Liquefaction Resistance Index (LRI) Zone. (a) Total number of pipes in each LRI zone, and areas of no liquefaction observations (NO). (b) Total pipe length (km) in each LRI zone, and areas of no liquefaction observations (NO). (c) Repair rates for each LRI zone, with standard errors indicated. Also shown are number of repairs (in *italics*) for each LRI zone.

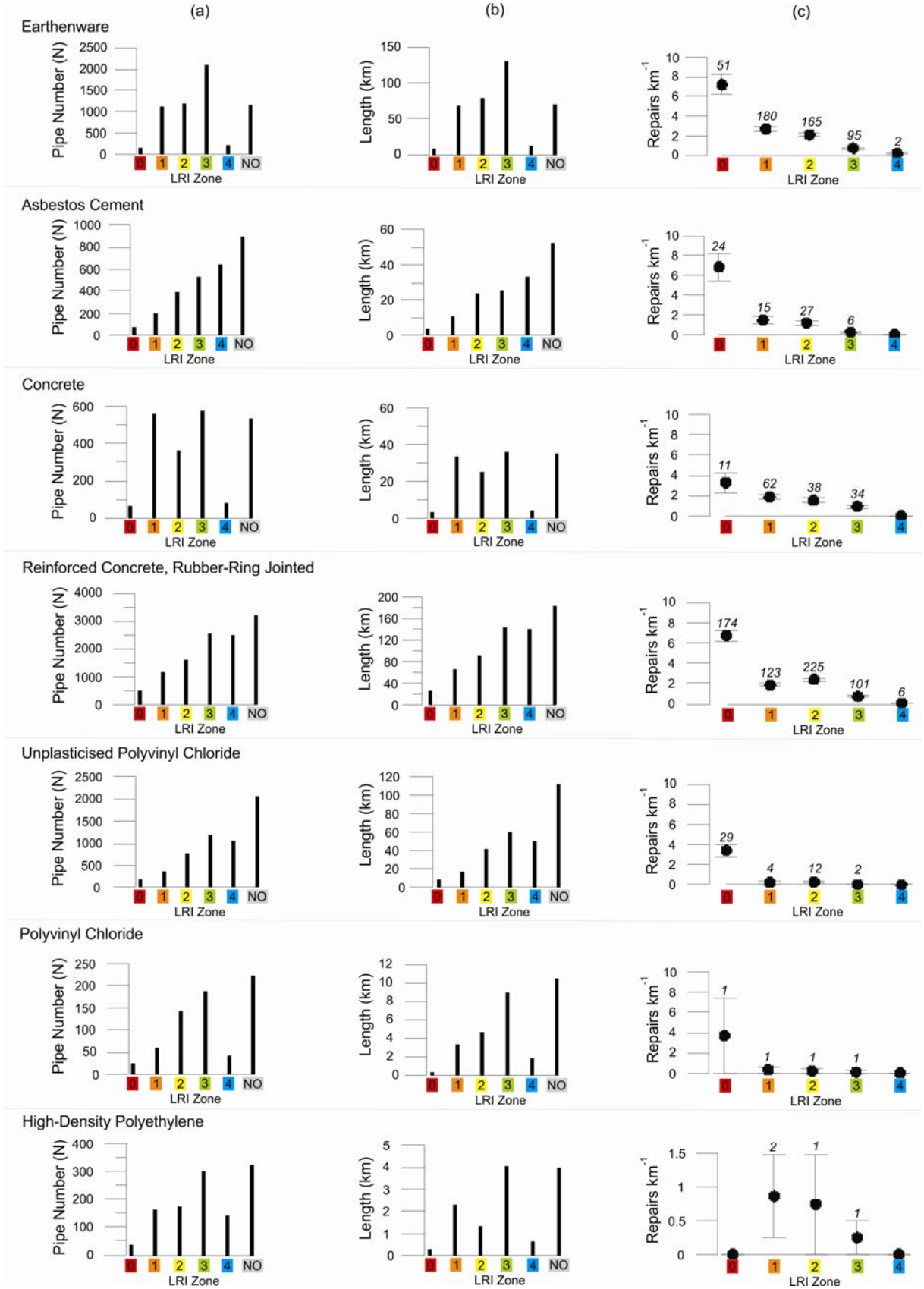

Figure 11. Wastewater repairs for each Liquefaction Resistance Index (LRI) Zone and pipe materials. (a) Total number of pipes in each LRI zone, and areas of no liquefaction observations (NO). (b) Total pipe length (km) in each LRI zone, and areas of no liquefaction observations (NO). (b) Total pipe length (km) in each LRI zone, and areas of no liquefaction observations (NO). (c) Repair rates for each LRI zone, with standard errors indicated. Also shown are number of repairs (in *italics*) for each LRI zone.

5.3 Roads

The damage to the road network of Christchurch was evaluated in the same manner as the pipe networks of the potable and waste water systems. For the road network three damage indicators were used: road 'failures' (cracks, fissures and vertical offsets), undulations resulting in uneven road surface, and uneven settlement or subsidence resulting in ponding of the roads. The summary analyses in terms of rates of failures, occurrences of uneven surfaces or ponding plotted against the LRI Zone are shown in Figures 12, 13 and 14.

Note that in many cases the data for the LRI Zone 0 is not representative for the performance of roads in this zone because majority of this zone was declared a Red Residential Zone and hence was outside the scope of damage evaluation and repairs. Having this potential anomaly in mind, by and large, the three datasets show consistent trend of increase in rates of damage features with a decrease in the liquefaction resistance of soils (or decrease in the LRI Zone number).

The data summary and interpretation also indicate that there is no significant difference in the performance of roads for different road surfaces. Further analysis of road performance is presented in Appendix B: Liquefaction Induced Damage to Roads in the 2010-2011 Christchurch Earthquakes.

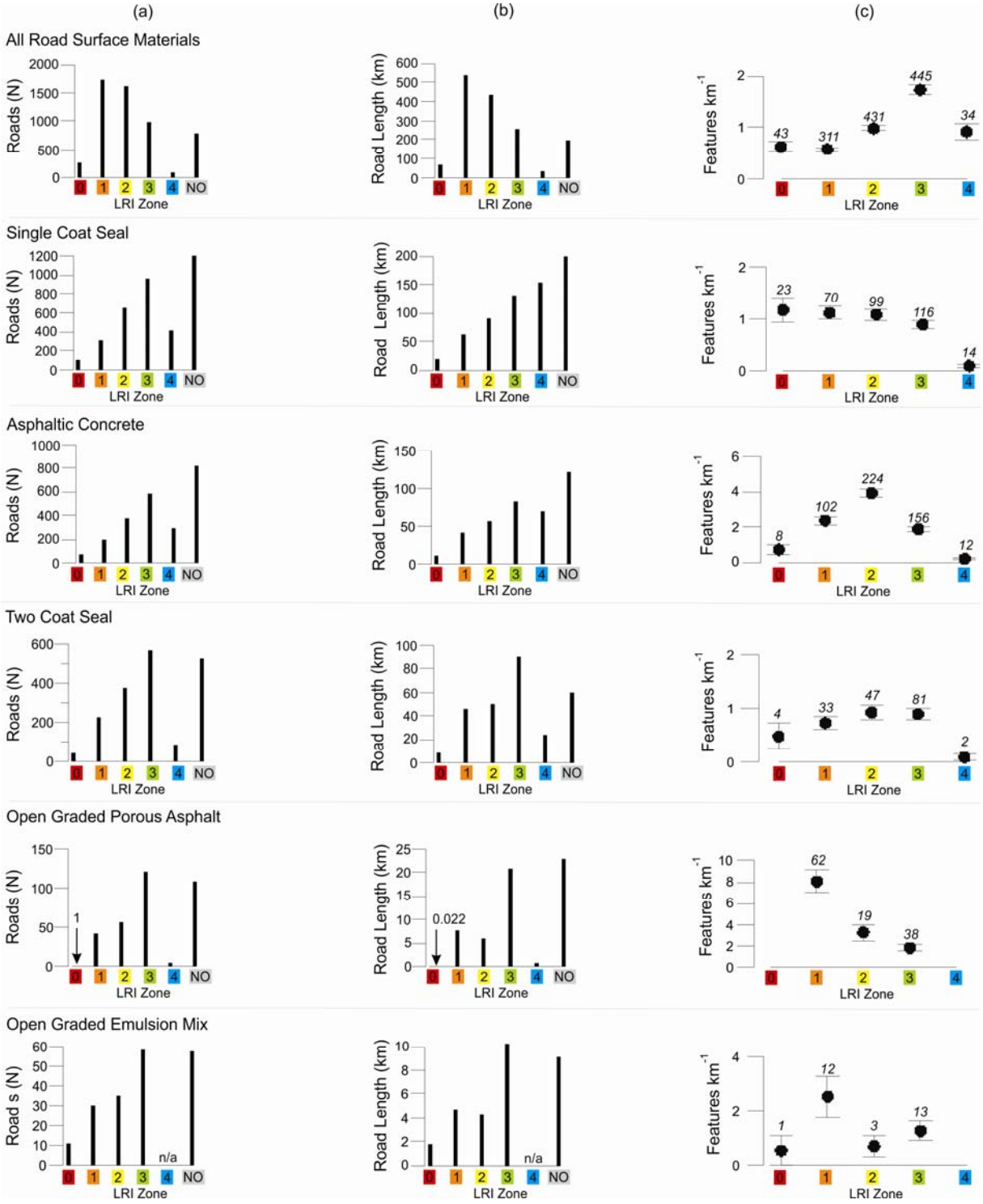

Figure 12. Road pavement damage observations (fissures, cracks, vertical offsets and potholes) across LRI zones. (a) Total number of roads in each LRI zone, and areas of no liquefaction observations (NO). (b) Total road length (km) in each LRI zone, and areas of no liquefaction observations (NO). (d) Rate of mapped features for each LRI zone, with standard errors indicated. Also shown are number of mapped features (in *italics*) for each LRI zone.

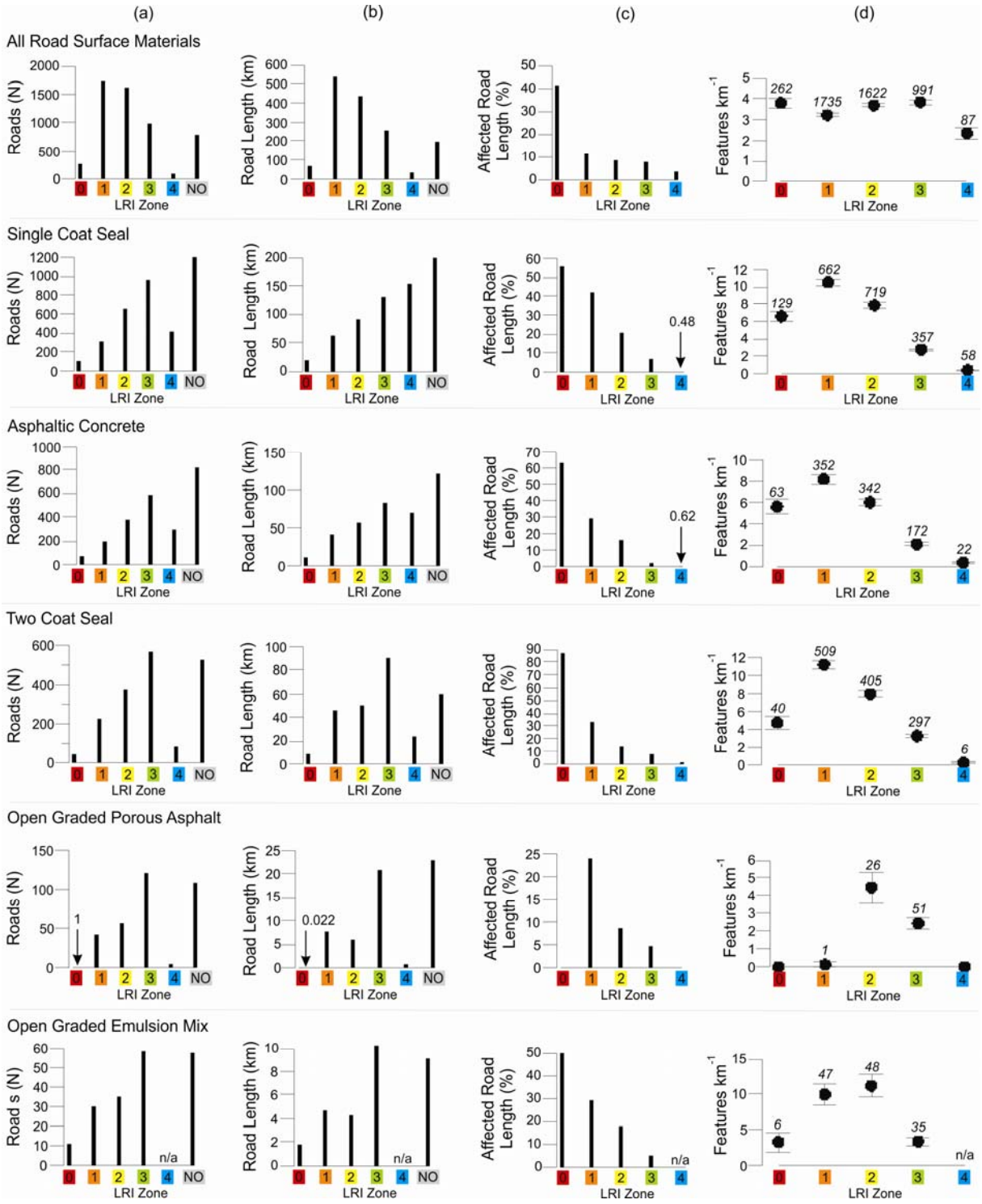

Figure 13. Road damage classified *uneven surface* for each Liquefaction Resistance Index (LRI) Zone and road surface material. (a) Total number of roads in each LRI zone, and areas of no liquefaction observations (NO). (b) Total road length (km) in each LRI zone, and areas of no liquefaction observations (NO). (c) Percentage of road length affected, classified as *uneven surface*, for each LRI Zone. (d) Rate of mapped features classified as *uneven surface* for each LRI zone, with standard errors indicated. Also shown are number of mapped features (in *italics*) for each LRI zone.

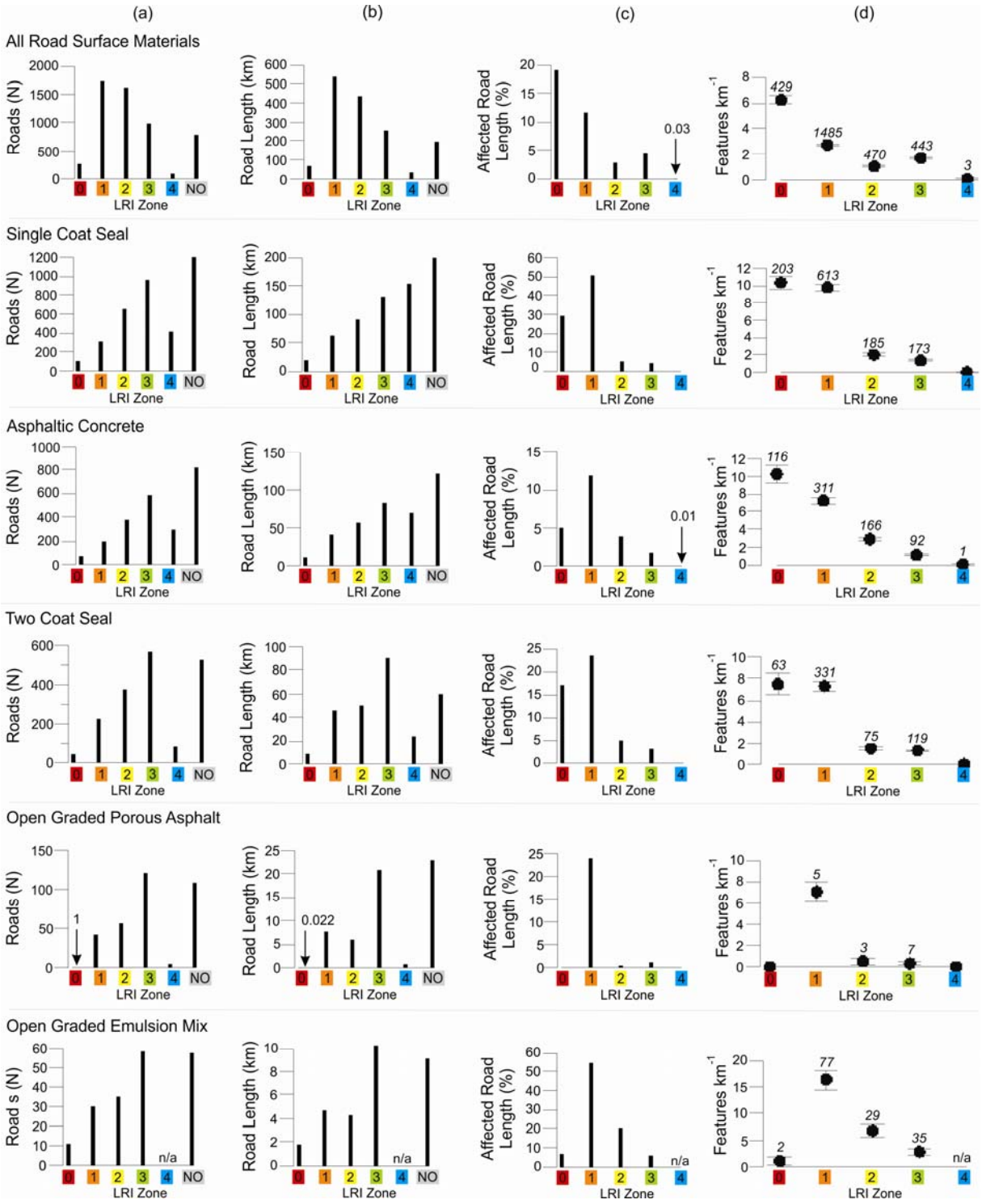

Figure 14. Road damage classified *ponding* for each Liquefaction Resistance Index (LRI) Zone and road surface material. (a) Total number of roads in each LRI zone, and areas of no liquefaction observations (NO). (b) Total road length (km) in each LRI zone, and areas of no liquefaction observations (NO). (c) Percentage of road length affected, classified as ponding, for each LRI zone. (d) Rate of mapped features classified and ponding for each LRI zone, with standard errors indicated. Also shown are number of mapped features (*in italics*) for each LRI zone.

6.0 Ongoing Analysis of the Waste Water System

The spatial distribution of waste water pipe types across Christchurch City is shown in Figure 15: the system is comprised dominantly of gravity pipes, with pressurised sections delivering waste water ultimately to the treatment plant at Bromley. Since the early 2000s, CCTV analyses of the gravity pipes in particular have been conducted as part of regular network assessment and maintenance (Figure 16a). Following 4 September 2010, CCTV inspections continued to determine the impacts of this event on the network (Figure 16b). Following the 22 February 2011 event and the formation of SCIRT as the primary horizontal infrastructure reconstruction organisation, an extensive programme of CCTV assessments was conducted to determine the extent and nature of waste water damage across Christchurch City (Figure 16c-e). As of May 2014, 53% of the network had been assessed with CCTV to determine structural damage, with 6% of this component also being assessed by profilometer to determine loss of grade (Figure 17). One percent of the network was assessed by profilometer only, to assess potential deformation and loss of grade of pipes comprised of ductile HDPE and PVC materials.

Based on specific criteria (SCIRT 2012; 2013), CCTV damage observations were classified by SCIRT into actions to be undertaken: renew (replacement of the entire pipe), repair (sections of a damaged pipe patched or replaced) or no action (Figure 18). A significant percentage of observations were abandoned, indicating that the CCTV survey had to be discontinued due to obstructions or pipe damage, both of which can often be attributed to earthquake effects. A large portion of the Residential Red Zone along the Avon River was unsurveyed, as this area was deemed unviable for future residential land use, and CCTV analyses were unnecessary. Final decisions on courses of action for specific pipes or groups of connected pipes were ultimately the responsibility of SCIRT design teams, who also incorporated profilometer and other site-specific information. While the CCTV data were not necessarily the final determinant of reinstatement actions, these data, supplemented by profilometer information, provide the most accurate assessment of pipe performance and physical damage in response to transient and permanent ground deformation. Fifty-four percent of Christchurch's waste water network has been assessed by either or both CCTV and profilometer, providing a picture of post-earthquake infrastructure performance unprecedented in detail.

A preliminary assessment of grade loss in selected areas of Christchurch is presented in Appendix A: Investigation in to the loss of grade of the Christchurch Wastewater Pipe Network after the 2010-11 Earthquakes. Liquefaction severity played a large role in influencing pipe movement and the extent of damage that observed. In terms of the performance of pipe materials, earthenware pipes suffered dips over a shorter length and it is speculated that cracks and/or joint failure resulted. Furthermore, UPVC pipes were found to have a much more flexible manner of movement and resisted cracking by subjecting a greater length of pipe to the dip displacement. In liquefaction-susceptible areas, there was a tendency for these pipes to suffer a loss of grade when their trench material consisted of locally excavated sands/soils. It was speculated that this is due to a 'floating effect' of the pipes in liquefiable soils. However, further analysis of the trench materials, such as AP20/AP40 mixtures, suggested that manhole movement in addition to liquefaction susceptibility result in a loss of grade of pipes.

Within SCIRT, assessment of the impacts of earthquake damage on the remaining lifetimes of gravity pipes has been investigated, with a methodology developed for assessing changes in remaining life

using a Likelihood of Failure process (Heiler and Apeldoorn, 2015). The Christchurch gravity network has sustained an average reduction in remaining asset life of approximately 20 years as a result of CES damage, with SCIRT repairs expected to return 15 years of remaining life to the network. Large diameter pipes have sustained a larger reduction in asset life than smaller pipes, and there will be further CCTV inspections of large diameter trunk to determine actual remaining asset life (Heiler and Apeldoorn, 2015). Because of the attendant economic implications of changes in asset lifetime for owners/managers, this is an emerging area of interest with significant implications for asset management and maintenance in Christchurch and across New Zealand.

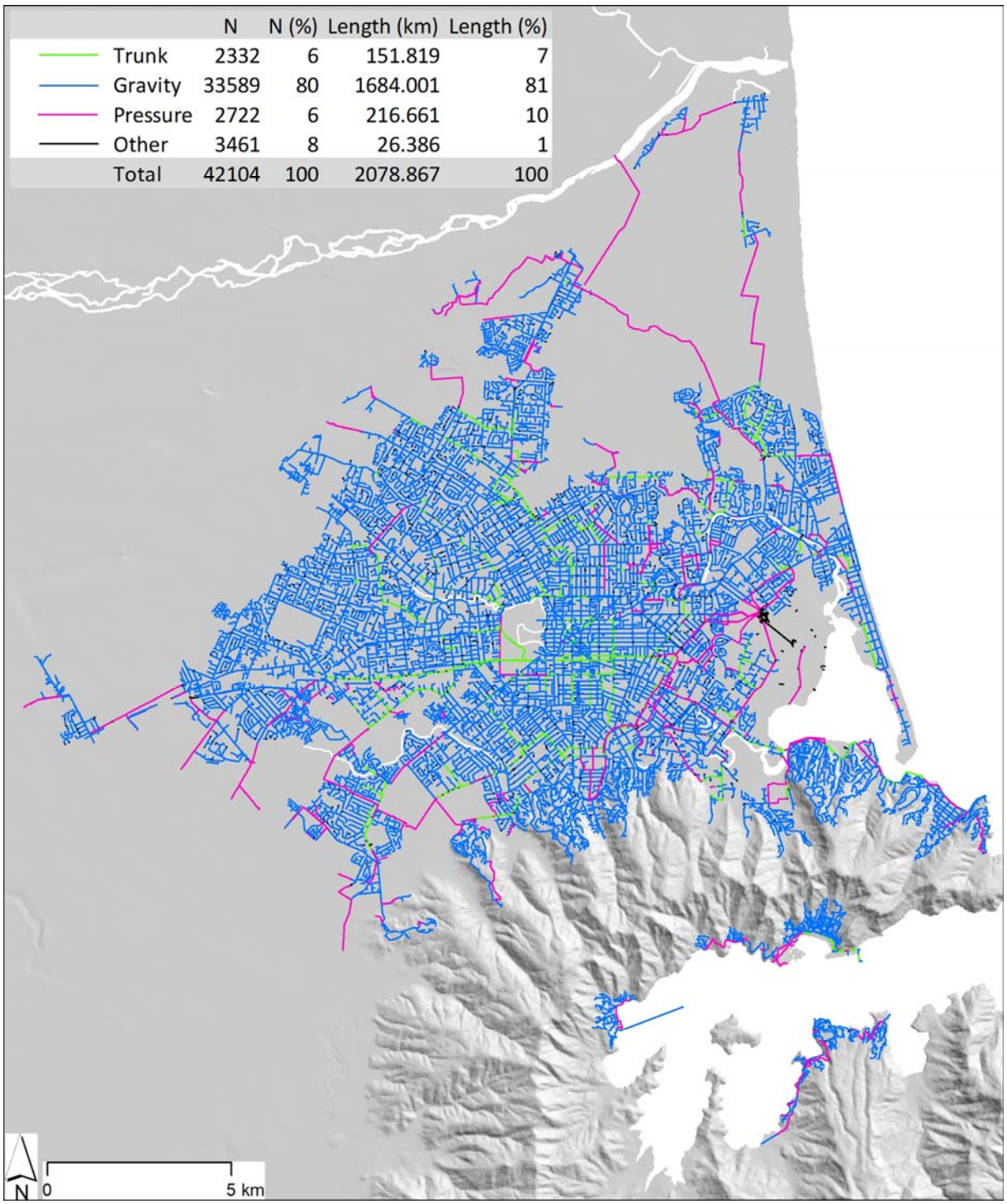

Figure 15. Waste water network pipe types across in Christchurch City and Lyttelton Harbour, as of 4 September 2010.

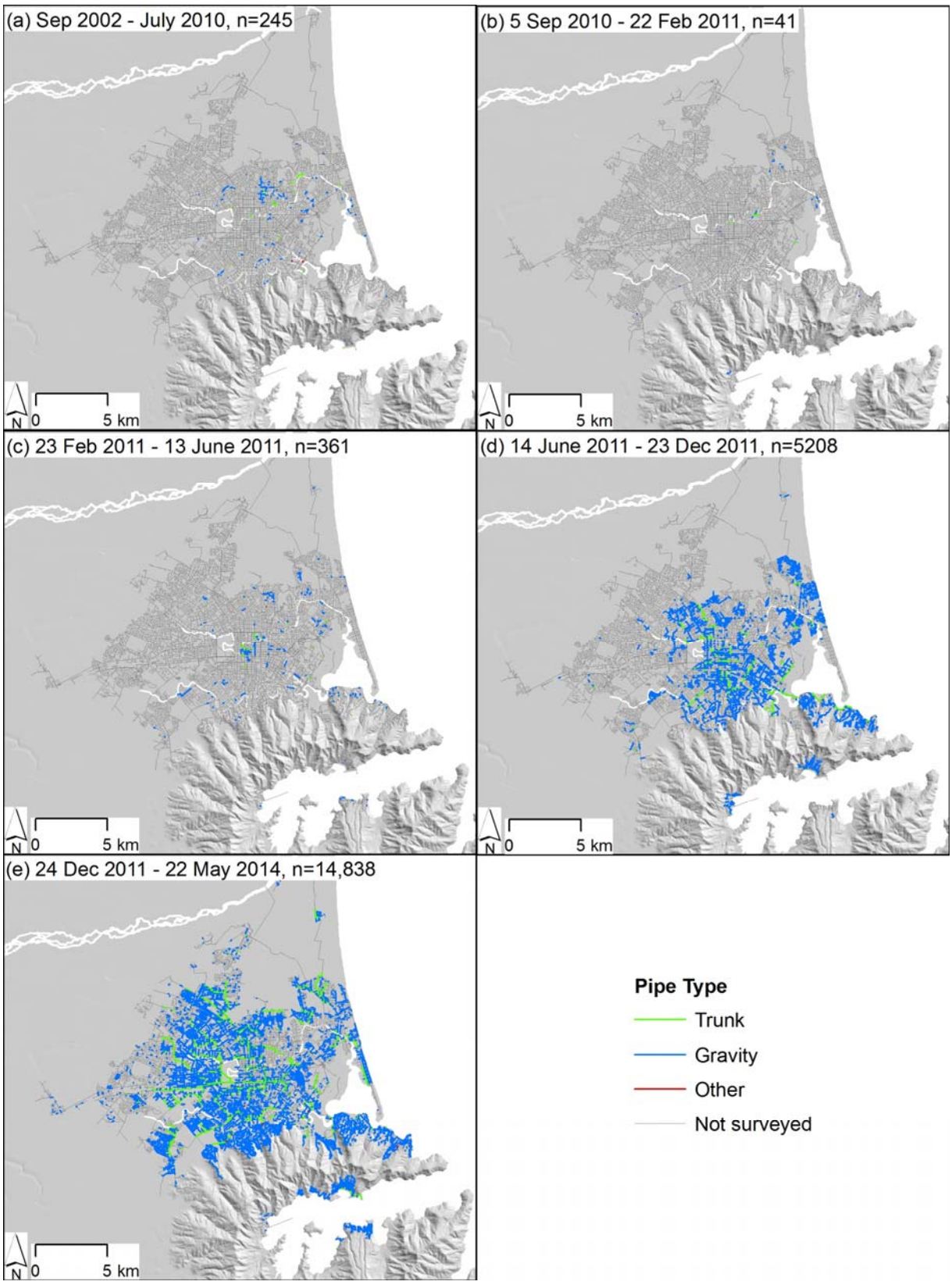

Figure 16. Locations of waste water CCTV analyses across Christchurch City and Lyttelton Harbour before the CES (a) and after each major CES event through to May 2014 (b-e).

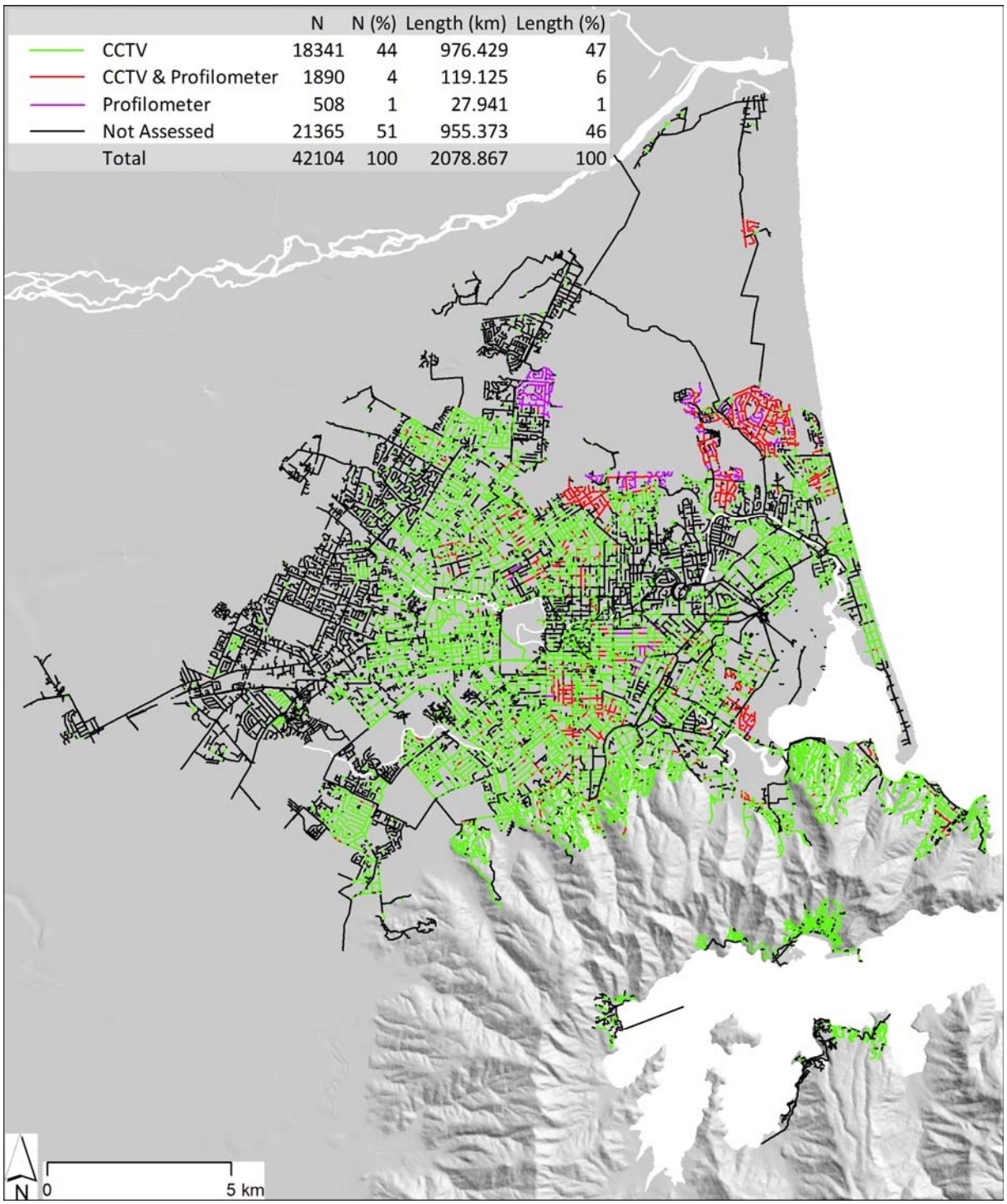

Figure 17. Post-CES locations of CCTV and profilometer observations across Christchurch City and Lyttelton Harbour.

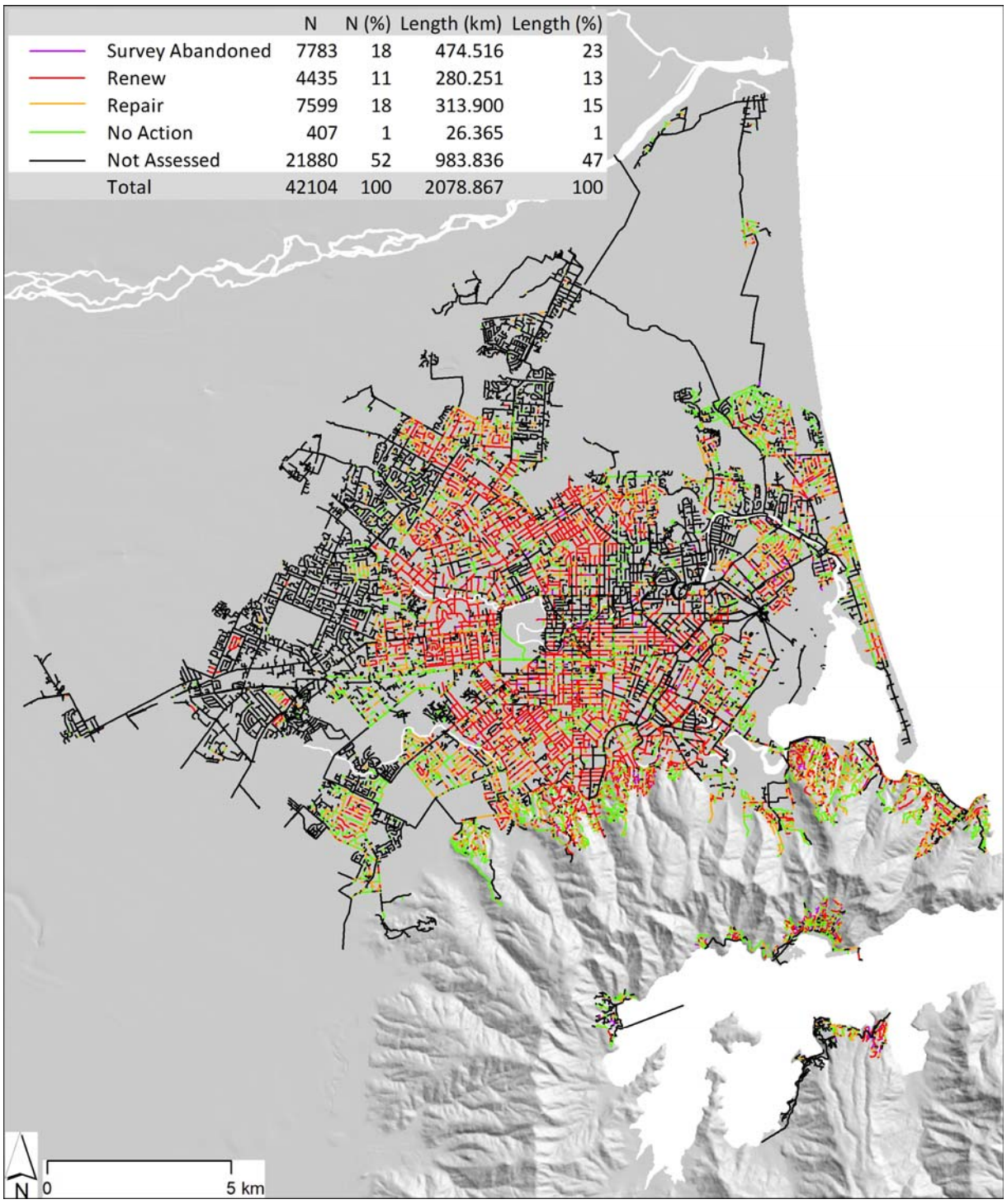

Figure 18. Assessment of actions (renew, repair, no action) for waste water pipes based on CCTV analysis. Survey Abandoned denotes CCTV surveys unable to be completed in the field due to pipe obstruction/damage.

The following is an overview of current and soon-to-be-started research on Christchurch's waste water system:

- Continuing analysis of waste water performance through the CES, based on CCTV data. Current work is assessing performance as determined by observed structural damage, and courses of action (renew, repair and no action) based on this physical damage. The influences of pipe material, age, embedment depth and trench fill material on performance are also being investigated.
- Correlation of network component performance with measures of seismicity and ground deformation. Specifically, CCTV structural damage observations from the 53% of Christchurch City's waste water network that has been surveyed (~20,000 pipes) comprise a voluminous and detailed record of earthquake impacts. Individual earthquake damage observations for the entire database will be geocoded for further spatial analysis, and correlated with PGA, PGV, $CSR_{(wt)}$ and $CSR_{7.5(wt)}$, and the LRI. Correlations with LiDAR-derived ground surface deformation as measured by vertical distortion and horizontal strain will also be conducted, in parallel with correlations with subsurface liquefaction behaviour using geotechnical observations/data.
- Production of damage curves based on correlations of observed physical damage with seismic and ground performance measures. Such curves will able to be incorporated in modelling platforms such as Riskscape, to assist asset managers in Christchurch, around New Zealand and internationally, to inform decision-making on improved system resilience. Such modelling approaches will need to be informed by local geotechnical conditions, and the expansion of the Canterbury Geotechnical Database in to the New Zealand Geotechnical Database will assist in more realistic site-specific modelling of system performance.
- Expansion of research on changes in remaining asset lifetimes resulting from earthquake impacts. More CCTV data from large diameter pipes will be captured, and the Likelihood of Failure methodology applied to this dataset to better inform Christchurch City Council's asset managers on pipe lifetime reductions. As the methodology is refined, guidelines will be developed to assist waste water asset managers in New Zealand and internationally to plan for and manage earthquake impacts.

References

Beavan, J., Fielding, E., Motagh, M., Samsonov, S., Donnelly, N., 2011. Fault location and slip distribution of the 22 February 2011 Mw 6.2 Christchurch, New Zealand, Earthquake from geodetic data. Seismol. Res. Lett. 82, 789–799. doi:10.1785/gssrl.82.6.789.

Beavan, J., Lee, J., Levick, S., Jones, K., 2012. Ground displacements and dilatational strains caused by the 2010-2011 Canterbury earthquakes. GNS Science Consultancy Report 2012/67, May 2012.

Beavan, J., Motagh, M., Fielding, E.J., Donnelly, N., Collett, D., 2012. Fault slip models of the 2010–2011 Canterbury, New Zealand, earthquakes from geodetic data and observations of postseismic ground deformation. New Zeal. J. Geol. Geophys. 37–41. doi:10.1080/00288306.2012.697472.

Beavan, J., Samsonov, S., Motagh, M., Wallace, L., Ellis, S., Palmer, N., 2010. The Darfield (Canterbury) Earthquake: Geodetic observations and preliminary source model. Bull. New Zeal. Soc. Earthq. Eng. 43, 228–235.

Bech, D., Cordova, P., Tremayne, B., Tam, K., Weaver, B., Wetzel, N., Parker, W., Oliver, L., Fisher, J., 2014. Common structural deficiencies identified in Canterbury buildings and observed versus predicted performance. Earthq. Spectra 30, 335–362. doi:10.1193/021513EQS028M.

Bradley, B., Hughes, M., 2012a. Conditional peak ground accelerations in the Canterbury earthquakes for conventional liquefaction assessment: Technical report prepared for the Department of Building and Housing - Part 2.

Bradley, B., Hughes, M., 2012b. Conditional peak ground accelerations in the Canterbury earthquakes for conventional liquefaction assessment: Technical report prepared for the Department of Building and Housing - Part 1. Christchurch.

Bradley, B.A., 2012. Strong ground motion characteristics observed in the 4 September 2010 Darfield, New Zealand earthquake. Soil Dyn. Earthq. Eng. 42, 32–46. doi:doi: 10.1016/j.soildyn.2012.06.004.

Bradley, B.A., Cubrinovski, M., 2011. Near-source strong ground motions observed in the 22 February 2011 Christchurch Earthquake. Seismol. Res. Lett. 82, 853–865. doi:10.1785/gssrl.82.6.853.

Bradley, B.A., Quigley, M.C., Van Dissen, R.J., Litchfield, N.J., 2014. Ground motion and seismic source aspects of the Canterbury Earthquake Sequence. Earthq. Spectra 30, 1–15. doi:10.1193/030113EQS060M.

Cubrinovski, M., Hughes, M., Bradley, B., McCahon, I., McDonald, Y., Simpson, H., Cameron, R., Christison, M., Henderson, B., Orense, R., O'Rourke, T., 2011. Liquefaction Impacts in Pipe Networks. Short Term Recovery Project No . 6. Natural Hazards Research Platform.

Cubrinovski, M., Hughes, M., Bradley, B., Noonan, J., Hopkins, R., McNeill, S., English, G., 2014a. Performance of Horizontal Infrastructure in Christchurch City through the 2010–2011 Canterbury Earthquake Sequence. Civil & Natural Resources Engineering Research Report 2014-02. University of Canterbury, March 2014. ISSN 1172-9511.

Cubrinovski, M., Hughes, M., O'Rourke, T.D., 2014b. Impacts of liquefaction on the potable water system of Christchurch in the 2010–2011 Canterbury (NZ) earthquakes. J. Water Supply Res. Technol. 63, 95–105. doi:10.2166/aqua.2013.004

Cubrinovski, M., Robinson, K., Taylor, M., Hughes, M., Orense, R., 2012. Lateral spreading and its impacts in urban areas in the 2010–2011 Christchurch earthquakes. New Zeal. J. Geol. Geophys. 55, 255–269. doi:10.1080/00288306.2012.699895.

Cubrinovski, M., Taylor M 2011. Liquefaction map of Christchurch based on drive-through reconnaissance after the 22 February 2011 earthquake, University of Canterbury.

Cubrinovski, M., Winkley, A., Haskell, J., Palermo, A., Wotherspoon, L., Robinson, K., Bradley, B., Brabhaharan, P., Hughes, M., 2014. Spreading-induced damage to short-span bridges in Christchurch. Earthq. Spectra.

Duffy, B., Quigley, M., Barrell, D.J.A., Dissen, R. Van, Stahl, T., Leprince, S., McInnes, C., Bilderback, E., 2012. Fault kinematics and surface deformation across a releasing bend during the 2010 Mw 7.1 Darfield, New Zealand, earthquake revealed by differential LiDAR and cadastral surveying. GSA Bull. 124, 420–431.

Fleischman, R.B., Restrepo, J.I., Pampanin, S., Maffei, J.R., Seeber, K., Zahn, F. a., 2014. Damage evaluations of precast concrete structures in the 2010–2011 Canterbury Earthquake Sequence. Earthq. Spectra 30, 277–306. doi:10.1193/031213EQS068M

Green, R. a., Cubrinovski, M., Cox, B., Wood, C., Wotherspoon, L., Bradley, B., Maurer, B., 2014. Select liquefaction case histories from the 2010–2011 Canterbury Earthquake Sequence. Earthq. Spectra 30, 131–153. doi:10.1193/030713EQS066M

Heiler, D., Apeldoorn, S., 2015. Assessing the impact of earthquakes on the remaining life of gravity wastewater pipes, in: Sustainable Communities - Sharing Knowledge. Rotorua, New Zealand. 7-11 June 2015.

Hughes, M.W., Quigley, M.C., van Ballegooy, S., Deam, B.L., Bradley, B.A., Hart, D.E., Measures, R., 2010. The sinking city : Earthquakes increase flood hazard in Christchurch , New Zealand. GSA Today 25, 4–10. doi:10.1130/GSATG221A.1.E-mails

Moon, L., Dizhur, D., Senaldi, I., Derakhshan, H., Griffith, M., Magenes, G., Ingham, J., 2014. The demise of the URM building stock in Christchurch during the 2010–2011 Canterbury Earthquake Sequence. Earthq. Spectra 30, 253–276. doi:10.1193/022113EQS044M

O'Rourke, T.D., Jeon, S.-S., Toprak, S., Cubrinovski, M., Hughes, M., van Ballegooy, S., Bouziou, D., 2014. Earthquake response of underground pipeline networks in Christchurch, NZ. Earthq. Spectra 30, 183–204. doi:10.1193/030413EQS062M

Quigley, M., Dissen, R. Van, Litchfi, N., Villamor, P., Duffy, B., Barrell, D., Furlong, K., Stahl, T., Bilderback, E., Noble, D., 2012. Surface rupture during the 2010 Mw 7.1 Darfield (Canterbury) earthquake : Implications for fault rupture dynamics and seismic-hazard analysis. Geology 55–58. doi:10.1130/G32528.1

Quigley, M.C., Bastin, S., Bradley, B.A., 2013. Recurrent liquefaction in Christchurch, New Zealand, during the Canterbury earthquake sequence. Geology 41, 419–422. doi:10.1130/G33944.1

Quigley, M.C., Hughes, M.W., Bradley, B.A., van Ballegooy, S., Reid, C., Morgenroth, J., Horton, T., Duffy, B., Pettinga, J., n.d. The 2010-2012 Canterbury Earthquake Sequence: Environmental Effects, Seismic Triggering Thresholds, and Geologic Legacy. Tectonophysics.

SCIRT, 2013. Infrastructure Recovery Technical Standards and Guidelines Version 4.3. Christchurch City Council, New Zealand Transport Agency, Canterbury Earthquake Recovery Authority.

SCIRT, 2012. Infrastructure Recovery Technical Standards and Guidelines Version 3.0. Christchurch City Council, New Zealand Transport Agency, Canterbury Earthquake Recovery Authority.

Tonkin and Taylor, 2013. Liquefaction Vulnerability Study.

Van Ballegooy, S., Malan, P., Lacrosse, V., Jacka, M.E., Cubrinovski, M., Bray, J.D., O'Rourke, T.D., Crawford, S. a., Cowan, H., 2014. Assessment of liquefaction-induced land damage for residential Christchurch. Earthq. Spectra 30, 31–55. doi:10.1193/031813EQS070M

Youd, T.L., Hansen, K.M., Bartlett, S.F., 2002. Revised multilinear regression equations for prediction of lateral spread displacement. J. Geotech. Geoenvironmental Eng. 128, 1007–1017.

Appendix A: Investigation in to the loss of grade of the Christchurch Wastewater Pipe Network after the 2010-11 Earthquakes

Investigation into the loss of grade of the Christchurch Wastewater Pipe Network after the 2010-11 Earthquakes

A. J. East and A. C. Lowe

Final Year Project, 2014
Dept. of Civil and Natural Resources Engineering
University of Canterbury
Project supervisors: M. Cubrinovski and M. Hughes

Keywords: *Wastewater network, liquefaction, earthquake damage, buried pipelines, GIS.*

ABSTRACT

The damage sustained by the Christchurch wastewater pipe network due to 2010-11 Canterbury earthquakes included the loss of grade of gravity operated pipes. As the majority (91%) of the network consists of gravity driven flow, this particular type of damage is of concern and is still poorly understood. The potential contributing factors to pipe dips include: liquefaction severity, pipe diameter, pipe material, pipe depth and trench backfill material. To investigate the occurrence of the dips, profilometer data provides an accurate measure of the dip severity and location. From the profilometer data, four assessment criteria were derived as a way to evaluate the pipes performance in terms of damage and serviceability. These four criteria were then applied to the chosen subset of pipes to determine a correlation with the damage observed. Through this analysis several conclusions were drawn and recommendations were made for future research in this field. Firstly, it was discovered that liquefaction severity plays a large role in influencing pipe movement and the extent of damage that is observed. In terms of the performance of pipe materials, it was found that earthenware pipes suffered dips over a shorter length and it is speculated that cracks and/or joint failure resulted. Furthermore, UPVC pipes were found to have a much more flexible manner of movement and resited cracking by subjecting a greater length of pipe to the dip displacement. An additional analysis was performed to assess the performance of trench materials. It was found that for pipes in liquefaction susceptible areas, there was a tendency for these pipes to suffer a loss of grade when their trench material consisted of locally excavated sands/soils. It was speculated that this is due to a 'floating effect' of the pipes in liquefiable soils. However, further analysis of the trench materials, such as AP20/AP40 mixtures, suggested that manhole movement in addition to liquefaction susceptibility result in a loss of grade of pipes. From the results obtained, further investigations have been proposed to validate the findings contained within this report.

1. INTRODUCTION

The 2010-11 Canterbury earthquakes resulted in extensive damage to the city's infrastructure and supporting lifelines. Damage to buildings and roads could be seen throughout the city and central business district, but what was not so evident was the extent of damage to the subsurface infrastructure. This damage resulted in many homes across the city being without potable water, power and wastewater services. Early estimates suggested that over 2 billion NZD would be needed to review and repair the damage incurred to the infrastructure which was predominately due to soil liquefaction and lateral spreading. Revised figures show that about 3 billion NZD would be needed to fully reinstate the horizontal infrastructure of Christchurch.

As a result of the topography of the Christchurch region, the majority (91%) of the wastewater network is gravity driven. The network consists of approximately 1,800 km of pipes which transport the wastewater to the Bromley treatment plant. Gravity pipes are laid in straight lines and at a constant gradient between access points (manholes and inspection chambers) (Cubrinovski, et al., 2011). The flatter grades, which these pipes are typically laid at, results in wastewater velocities that are lower than the traditionally used self-flushing velocity of 0.7 m/s. Due to this, the network works in conjunction with a large number of pumping stations.

Wastewater pipes are typically laid at depths between 2.0 and 3.5 m with a minimum vertical cover of 1.2 m. For this reason, repairs to network are not only more difficult but are generally economically driven. The ground motion induced by the earthquakes made the network susceptible to various types of damage including a loss of grade. This has led to a damage classification known as 'pipe dipping.' This is where a section of pipe has locally settled resulting in a dip with a positive grade along the pipe in a direction opposite to the intended gravity driven flow.

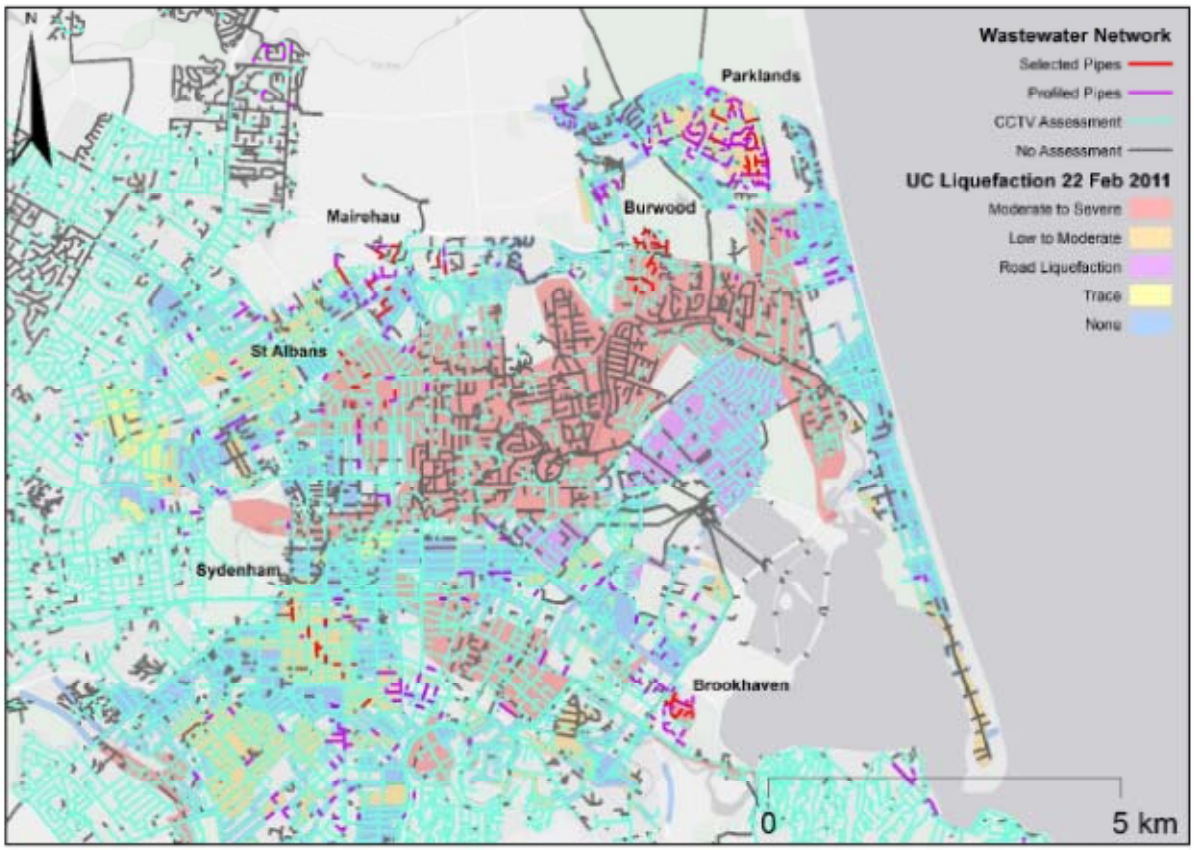

Figure 1. Spatial representation of the profiled wastewater pipes in Christchurch laid over the liquefaction severity map as generated by Cubrinovski & Taylor, 2011.

This particular type of damage is still poorly understood with uncertainty behind the contributing factors to the pipe dips. Along with others, the list of potential factors includes: liquefaction severity, pipe diameter, pipe material, pipe depth and trench backfill material. A recent study (Cave, 2013) was unable to identify a clear correlation between trench material and pipe dipping. However, with more profilometer data of pipes across the city now available, this area of research has been revisited with the intention of identifying the key factors that contribute to pipe dips.

For this investigation, profilometer data was acquired courtesy of the Stronger Christchurch Infrastructure Rebuild Team (SCIRT) in order to assess the pipes. A spatial representation of the profiled pipes in the city can be seen in Figure 1 with the liquefaction severity zones in the background.

2. PIPE CONDITION ASSESSMENT BY SCIRT

Investigations of the wastewater network by SCIRT thus far have included a CCTV assessment of approximately 48% of pipes in the Christchurch system. These pipes were chosen based on the expected damage of brittle natured pipes and observed land damage after the earthquake events. A CCTV assessment involves feeding an inspection camera through the pipe as a visual assessment of its condition. From the CCTV footage, as of October 2014, 6% of these assessed pipes were deemed to have a level of pipe dipping greater than 30% of their respective diameter as set out by the Infrastructure Recovery Technical Standards and Guidelines (IRTSG). For these pipes, a profilometer survey was conducted to more accurately measure the dips observed and to determine the type of action (renewal, repair or no action) required for the pipe. The following statements can be made about this information:

- If a pipe has been profiled it has suffered above moderate levels of damage and requires either a discrete repair or renewal.
- If a pipe was not profiled it may have suffered some other form of damage (i.e. cracks) but not a level of dipping greater than 30% of its diameter; or the pipe suffered no damage.

At the inception of this investigation in February 2014, the total number of profiled pipes in the network was 542; this is approximately 1.4% of the total network. From these, 103 pipes were selected to form a subset of data from which this investigation is based on. These pipes were selected to encompass the three most dominant pipe materials (UPVC, earthenware and

reinforced concrete) in the most prevalent liquefaction severity zones.

An interesting point of discussion is the lack of profiled pipes in the moderate to severe and road liquefaction zones on Figure 1 above. The figure shows that some pipes in these areas have had a CCTV assessment but not been profiled. The explanation for this is that either these pipes suffered no damage or were so extensively damaged that they were repaired or replaced immediately; the latter is more probable. The regions with a considerable lack of CCTV and/or profilometer assessments are where the Canterbury Earthquake Recovery Authority (CERA) have deemed the 'red zone'. As stated in the IRTSG (2013): 'As a general principle, existing services through the red zone should be abandoned rather than repaired.'

3. METHODOLOGY

3.1. Acquired Information

Wastewater Network Data

At the commencement of this investigation, a GIS database of the Christchurch wastewater network provided the attribute information for all wastewater pipes and manholes throughout the city.

Profilometer Data

As defined by Yukich (2013), 'A profilometer is a level sonde that is pulled through the pipe (typically from downstream manhole to upstream manhole), recording the elevation of the sonde in relation to a base station at specified intervals, typically one metre.' A horizontal profile of the pipe invert can then be generated from the profilometer recordings. The profile plot is then used to show the location and severity of dips along the pipe.

The subset of data chosen for this investigation covers a range of areas in Christchurch that experienced a variety of liquefaction severities as defined by the liquefaction severity map. In addition to this, the subset covered the three materials that make up the majority of the wastewater network: unplasticised polyvinylchloride (UPVC), reinforced concrete rubber ringed (RCRR) and earthenware (EW). The distribution of the selected pipes can be observed below in Table 1.

Table 1. Selected areas in Christchurch and the corresponding data attributes.

Area	No. of Pipes	Liquefaction Severity Zone	Material(s)
Brookhaven	12	Moderate to Severe	UPVC and EW
Burwood	24	Moderate to Severe	RCRR and UPVC
Mairehau	21	None	RCRR and UPVC
Parklands	24	Low to Moderate	UPVC and EW
St Albans	8	Moderate to Severe	EW
Sydenham	14	Low to Moderate	EW

In determining the potential causes of dips in pipes, simple intuition alluded to liquefaction severity as being a primary contributor to the observed damage. For this reason, it was necessary to obtain an indication of the liquefaction severity throughout the city. It was decided to assess the pipes in relation to the liquefaction severity map produced by University of Canterbury (UC) staff. The map (Cubrinovski & Taylor, 2011) was generated after a drive-through reconnaissance survey that was conducted across the city after the 22 February 2011 event. This is shown in the background of Figure 1 with the zones defined as:

(a) moderate to severe liquefaction (with very large areas covered by sand ejecta, mud and water, larger distortion of ground and pavement surfaces, large fissures in the ground, and significant liquefaction-induced impacts on buildings and infrastructure), (b) low to moderate liquefaction (with generally similar features as for the severe liquefaction, but of lesser intensity and extent), (c) liquefaction predominantly on roads with some on properties (where heavy effects of liquefaction were seen predominantly on roads, with large sinkholes and 'vents' for pore pressure dissipation, and limited damage to properties/houses), and (d) traces of liquefaction, but limited in extent and deemed not damaging for structures) (Cubrinovski, et al. 2011).

3.2. Assessment Criteria

To gain an understanding of the wastewater pipe's performance after the earthquakes and to assess the extent of the pipe dips, several criteria have been obtained or derived. These criteria were used as an aid in evaluating the pipes in terms of damage and effects on serviceability. The four criteria established for this investigation are defined and quantified as follows. The definitions of the criteria are based off aspects of the profilometer plots. An example profilometer plot is shown in Figure 2 with the associated criteria designations.

SCIRT Dip Criterion (SDC)

This criterion has been attained from the dip categories specified in the New Zealand Pipe Inspection Manual (NZPIM). These categories were revised by SCIRT in their Profilometer Designer Guideline to align with the categories set out in the Infrastructure Recovery Technical Standards and Guideline (IRTSG). Hence the criterion was aptly named the SCIRT Dip Criterion (SDC) for the purpose of this investigation.

This criterion can be defined as the ratio of the dip height and pipe diameter, as a percentage. Where the dip height, ΔH, is determined as the difference between the local dip maximum and minimum as observed on Figure 2. The SDC value for each dip is calculated from the following expression:

$$SDC = \frac{\Delta H}{D} x100 \quad (in\ \%)$$

where D is the pipe diameter. From the SDC value determined, the pipe dips are then classified according to the 'traffic-light' categories presented in Table 2.

Table 2. SDC dip categories.

Dip Category	SDC (%)
Small	<30
Medium	≥30-<50
Large	≥50

Loss of Grade Index (LGI)

It was recognised that a deficiency with the SDC is that it does not take into account the length over which the dip occurs. Therefore, the Loss of Grade Index (LGI) was developed with the intention of incorporating the dip length. Similarly to the SDC, this criterion uses the height of the dip, ΔH, but determines its gradient by dividing the dip height by its length, ΔL. The length of dip is defined in Figure 2. LGI is calculated using the following expression:

$$LGI = \frac{\Delta H}{\Delta L} x100 \quad (in\ \%)$$

The values are classified according to the 'traffic-light' categories presented in Table 3. These threshold values were selected based on observations from the profilometer plots. Typically, the gradients observed ranged between 0.2% and extreme values such as 7%. These different gradients will impart different levels of stresses depending on how the pipe materials react. Hence, the 1% and 3% thresholds were assigned arbitrarily to the categories to give an indication of the severity of the gradient.

Table 3. LGI dip categories.

Gradient Category	LGI (%)
Shallow	≤1
Moderate	>1-≤3
Steep	>3

Whole Length Gradient (WLG)

This criterion, as the name suggests, investigates the overall gradient from manhole to manhole, evaluating its serviceability. It then compares this to the minimum downstream grades set out in the Infrastructure Design Standard (6.5.5 - Minimum gradients (Table 3)). These minimum gradients, for the respective pipe diameters are shown in the Table 4.

Table 4. Minimum downstream gradients from the IDS.

Diameter (mm)	Minimum Gradient
150	1/350
175	1/400
200	1/450
225	1/450
>300	1/500

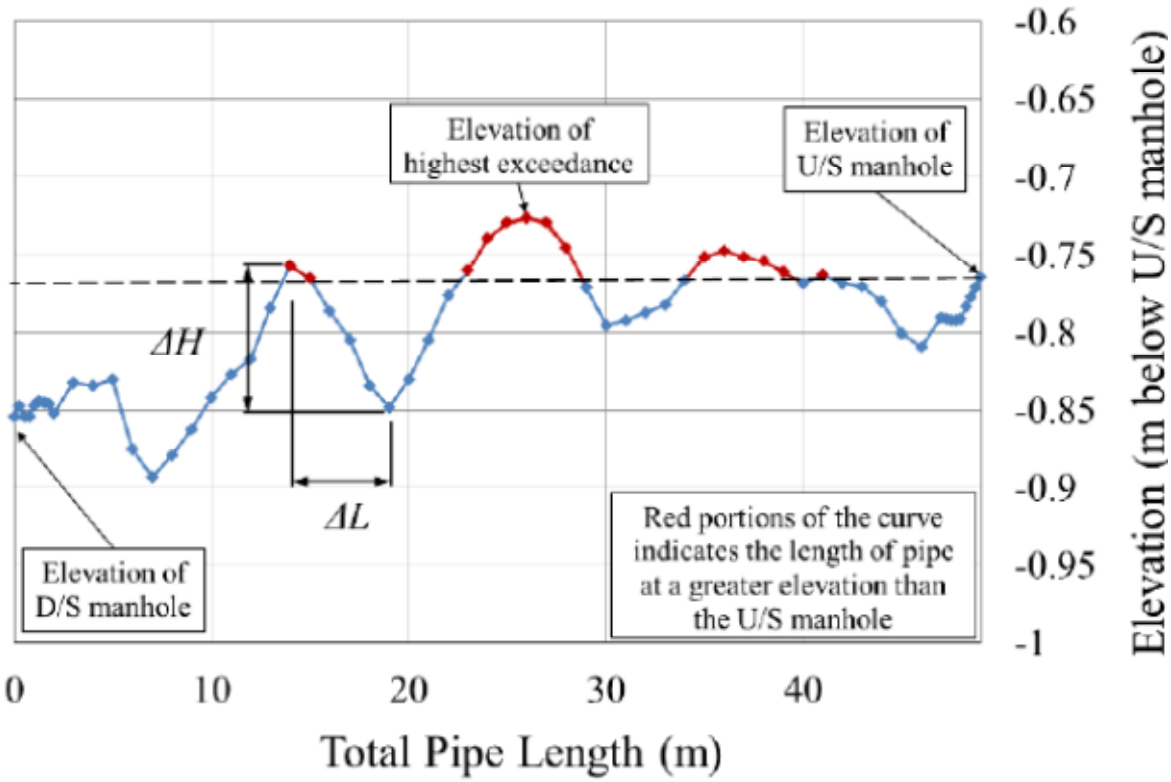

Figure 2. Sample profilometer plot showing the necessary criterial information.

The whole length gradient of the pipe is calculated from the ratio of the elevation difference between the upstream and downstream manholes, and the total pipe length, as observed in Figure 2. This gradient is then divided by the minimum gradients from Table 4 to determine if the pipe has a steeper or shallower gradient than the minimum standard. If the ratio of the gradients has a value equal to or greater than one then the pipe gradient is steeper than the allowed minimum. For WLG values less than one, the pipe gradient is not sufficient and hence this criterion is not satisfied.

Backwash Potential

The final criterion that was used to assess the performance of the wastewater pipes again focusses on a potential serviceability issue. Named the Backwash Potential, this criterion investigates the likelihood that the flow of wastewater will be impeded by an uplift of the pipe. With reference to basic fluid mechanics, fluid will tend to flow in the direction of less head. Therefore, any points along the pipe that are at a greater elevation than the upstream manhole elevation will impede the flow. This increases the potential for ponding along the pipes and in manholes and for backwash of wastewater.

From this criterion it is desired to know the total length of pipe and hence the volume within the pipe that is above the upstream manhole. From Figure 2, it can be seen that two metres adjacent to both upstream and downstream manholes, the profilometer points are at 25 cm intervals; whereas, the remaining pipe length is profiled at one metre intervals. The number of points above the upstream manhole is then converted to a length using the abovementioned intervals.

The volume of pipe above the upstream manhole is then calculated by multiplying this length by the cross-sectional area of the pipe (i.e. a function of its diameter). For the purposes of this investigation, it has been decided that any amount of pipe volume that exceeds the upstream manhole elevation is detrimental to its serviceability as theoretically no fluid should occupy this volume. Therefore, a simple pass-fail criterion has been adopted to whether any volume exceeds the upstream manhole elevation. In reference to Figure 2, the portion of the pipe coloured red indicates the length of pipe of which the volume is calculated from. It is this volume that will cause backwash, and consequently ponding.

4. RESULTS AND ANALYSIS

To get an understanding of the data that was available, a simple analysis was initially performed to assess how many of the damaged pipes were within the various liquefactions severity zones. Furthermore, the percentages of each pipe material that were effected is shown in Tables 5. The table shows that a third (33.2%) of the damaged pipes were in the low to moderate severity zone. The next largest quantity of damage was in the 'none' liquefaction severity zone with 28.6% of the total profiled pipes. An ambiguous result is that only 15.5% of damaged pipes were in the moderate to severe liquefaction severity zone. This may seem like an incorrect result, however, as observed in Figure 1, a large portion of the moderate to severe zone was not considered in the assessment by SCIRT. This is because this area was severely impacted by liquefaction and lateral spreading damage and has hence been classified as the abandoned 'red zone'.

By excluding this area in the analysis, the results become somewhat biased towards the other liquefaction zones. If pipes were assessed in this excluded area, it is expected that there would be extensive damage to the network. This would result in a larger proportion of damage being observed in the moderate to severe zone compared to the other zones. The results from this analysis would then follow a more expected trend which is: as liquefaction severity increases, the damage incurred by wastewater pipes increases.

From Table 5, it can be observed that the majority (78.8%) of dip related damage occurred in EW, RCRR and UPVC pipes. This is expected as these materials make up the majority of the pipe materials in the network. A more interesting point is that 41% are UPVC which is the predominant material used for the wastewater pipes these days. Dips occurring in these pipes could be due to the fact the UPVC is a more ductile material. In conjunction with socketing joints, this allows some relative movement between pipe segments resulting in more flexibility compared to earthenware or reinforced concrete pipes.

Table 5. Distribution of pipe materials in the liquefaction severity zones.

		Liquefaction Severity Zone						
		Moderate to Severe	Low to Moderate	Trace	None	No Zone	Total	Percent (%)
Material	AC	0	22	0	15	4	41	7.6
	CI	1	1	0	0	1	3	0.6
	CLS	0	0	0	0	1	1	0.2
	CONC	6	2	1	6	3	18	3.3
	EW	12	38	1	22	7	80	14.8
	HDPE	1	3	0	9	6	19	3.5
	MDPE300	0	0	0	2	2	4	0.7
	PE	0	0	0	2	0	2	0.4
	PVC	3	11	0	9	4	27	5.0
	RCRR	26	25	7	48	19	125	23.1
	UPVC	35	78	2	42	65	222	41.0
	Total	84	180	11	155	112	542	100.0
	Percent (%)	15.5	33.2	2.0	28.6	20.7	100.0	

A table, similar to Table 5, was produced to observe the distribution of diameters in each liquefaction zone. It was found that 75.6% of the damaged pipes have a diameter of 150 mm. Again, this result is expected as approximately 60% of the network's pipes are 150 mm in diameter. This distribution of diameters has implications to the analysis as there is a lack of data representing the other diameters. For this reason, conclusions on the performance of certain diameters based on percentages will perhaps be biased as there is an uneven distribution of diameters. After extensive discussions with several SCIRT engineers, scrutinising the effect of different diameters as cause for the dips is difficult. This is due to the lack of viable data available for pipe diameters greater than 300 mm hence resulting in an uneven distribution.

The analysis then focussed on assessing the pipes in terms of the four criteria developed. In particular SDC and LGI were used to assess the damage to the pipes in relation to their materials. For the selected pipes many of the profilometer plots exhibited one, two or three dips along the pipe length. The three most severe dips for each pipe were investigated and hence the total number of dips that occurred in the 103 selected pipes was 214 dips. Each of these dips was assigned an SDC and LGI value. Shown in Table 6, the total number of dips for each associated category is displayed in their respective suburbs. For the SCIRT Dip Criterion, it can be seen that 23% of the dips occur in the large dip category. The majority of this comes from dips occurring in Parklands, Burwood and Brookhaven; areas that have low to moderate and moderate to severe liquefaction severities respectively. Furthermore, the lowest contribution to large dips, according to the SDC, comes from Mairehau and Sydenham which are in none and low to moderate liquefaction severity zones respectively.

Table 6. Total number of dips in their respective category for the case study areas.

			Suburb						
			Brookhaven	Burwood	Mairehau	Parklands	St Albans	Sydenham	Percent (%)
Assessment Criteria	SDC	<30%	16	32	25	12	3	8	45
		30-50%	6	17	10	17	5	13	32
		>50%	6	12	4	19	5	4	23
	LGI	<1%	12	31	21	13	4	7	41
		1-3%	10	23	15	29	6	9	43
		>3%	6	7	3	6	3	9	16

In reference to the LGI figures of Table 6, the proportion of steeper dips in its respective suburb subsets is largest in Sydenham followed closely by St Albans and Brookhaven, all of which are earthenware pipes. Upon inspection of the profilometer plots for these pipes, the profiles showed a steep negative grade mirrored by the steep positive grade over a short distance; much like a 'V' shape. By then referring to CCTV log sheets, one discovered that the location of the 'V' dips coincided with either longitudinal, circumferential or a combination of cracks. It is also likely these dips occurred due to a joint failure during bending distortions associated with ground movement. Due to the nature of the profilometer data, there is uncertainty to whether the dips occur at the joints or in the span of the pipes. However, intuitively it would be expected that during bending, the joints would be the most vulnerable to deformation. Furthermore, as EW pipe segments, typically 2 m, are shorter than UPVC segments (6 m) this will induce dipping over shorter lengths.

Following this, an attempt was made to determine if there is any correlation between SDC and LGI for the dips. As mentioned earlier, each dip has an associated SDC and LGI value which can be plotted together. To get an understanding of the different materials behaviour, the SDC vs LGI plots shown in Figure 3 were separated into the various materials.

It should be addressed first that the number the dips that occurred in UPVC is 107, whereas for EW and RCRR the numbers of dips is 56 and 51 respectively. This could be due to an uneven distribution of pipe materials investigated: 49, 31 and 23 respectively for Figure 3 a), b) and c).

An initial observation of the plots alludes to no obvious correlation between SDC and LGI. However, a general trend between all plots shows a reoccurring cluster of points in the lower left corner of the plot area. For UPVC, approximately 80% of points occur below 3% LGI. It has been theorised that as UPVC is of a more flexible nature, when a dip occurs, a larger length of pipe is subjected to a change in gradient when the pipe moves in the direction of the dip. As a result, the dip length is much greater, thus generating a smaller LGI value. The ductile behaviour of UPVC pipes means that it is more prone to bending of large lengths rather than smaller, localised failures/ curvatures.

It is expected that RCRR pipes will perform similarly to EW, that is, rigid behaviour with brittle failures (cracks) along the pipe and at joints. While the abovementioned has been speculated through investigational evidence, this phenomenon may well be an intrinsic property for these brittle natured materials. However, it could also be a direct consequence of limited data and should be further investigated to validate this claim.

a) UPVC pipes in all areas and liquefaction zones

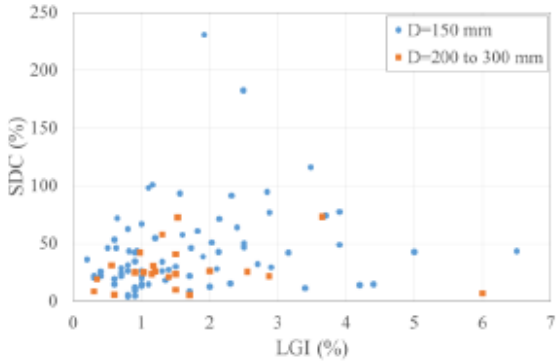

b) EW pipes in all areas and liquefaction zones

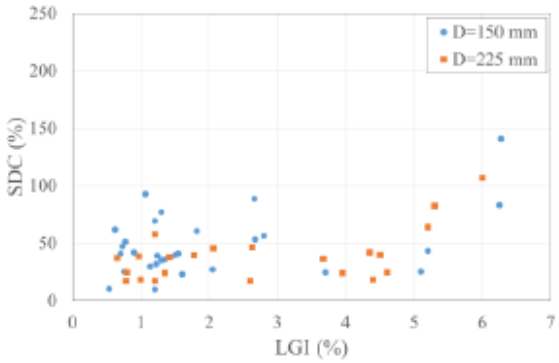

c) RCRR pipes in all areas and liquefaction zones

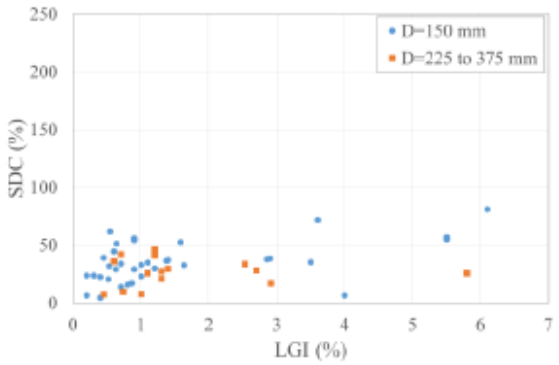

Figure 3. Comparison of materials plotting SDC against LGI for all areas and liquefaction zones.

Another factor that was believed to have caused loss of grade in the network was the interaction of the pipe with the trench backfill material that it is embedded in. Table 7 below, is a summary of the trench backfill materials used in terms of their location and year of installation. Locally excavated soils consist of Kaiapoi fine sandy loam, Taitapu silt loam and Waimari peaty loam. Similarly, locally excavated sands consists of various deep sandy and silty loams such as Aranui complex.

Table 7. Trench backfill materials based on the year of instalment in their associated regions.

Year	Location	Backfill Material
1880 - 1945	City Wide	Locally excavated soils
1940 - 1960	Eastern Suburbs	Locally Excavated sands
1946 - 1959	Central & Western Suburbs	Locally excavated soils
1960 - 1990	City Wide	CDB Spec (AP20/AP40)
1990 - Present	City Wide	CCC CSS Spec (AP20/AP40)

It was then decided to assess the four trench materials against the WLG and Backwash Potential criteria. This was to assess the serviceability performance of each backfill material. For the WLG criterion shown in Figure 4, it can be observed that the locally excavated sand had the largest proportion of failures. Table 7 indicates that locally excavated sands are used only in the eastern suburbs where the most severe liquefaction occurred and where there are very shallow water table depths. Saturated sand, being a highly dilative material, is most susceptible to liquefaction. Consequently, pipe and manhole movement as well as the WLG value is highly influenced by liquefaction. It has been observed through profilometer plot analysis that some pipes in liquefiable soils act in a buoyant manner in the presence of liquefaction causing a floating effect. However, it cannot be said with certainty that this floating effect is due to the uplift of the pipe or settlement of the manholes and is worth further investigation. This uncertainty is further reinforced by interpreting Figure 5. The figure shows that the newer trench material (AP20/AP40) had larger proportions of Backwash Potential failures than the locally excavated sands/soils. It is expected that the AP20/AP40 will not liquefy based on its composition (gravels and fines). Hence the reason why there is a larger proportion of failures for these trench materials could be due manhole movements which result in the pipe appearing like it has floated.

While the abovementioned is coherent across all trench materials, special consideration should be given to the fact the distribution of trench material data is unevenly distributed across the 103 pipes that have been selected. As a result it should be acknowledged that these results are potentially biased.

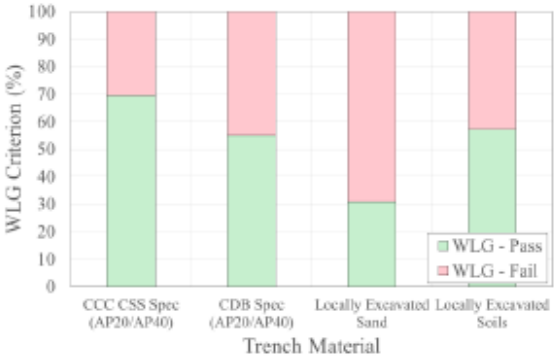

Figure 4. Performance of trench materials to the Whole Length Gradient criterion.

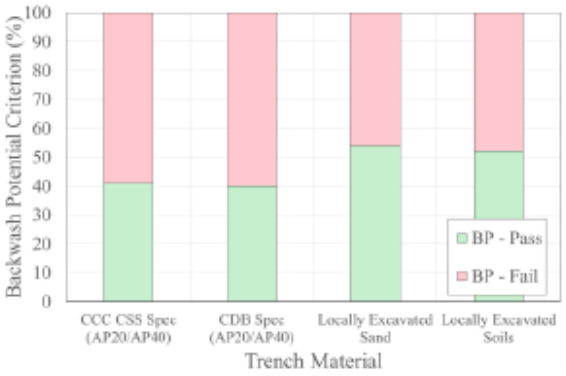

Figure 5. Performance of trench materials to the Backwash Potential criterion.

5. CONCLUSIONS AND RECOMMENDATIONS

At the commencement of this project, the overall aim was to identify the factor(s) that contribute to the loss of grade of pipes in the wastewater network. Throughout the investigation, the complexity of this aim became evident due to the type of data provided and the intricate nature of empirical research.

While no clear correlation of factors were identified from the analyses that were performed, several validated investigational conclusions were drawn as stated below. In addition to this, several recommendations for continuing research in this field are:

- An important outcome from this investigation was the four assessment criteria there were derived. These criteria, and their associated thresholds, give a way of assessing pipes and an indication of the pipes performance in terms of both damage and serviceability.
- Liquefaction severity plays a large role in influencing pipe movement. In particular, the interaction between liquefaction and pipe material presented some useful insight. From the profilometer data of the 542 pipes, rigid-like materials such as EW and RCRR displayed dips occurring over shorter lengths, i.e. localised failures; whereas, UPVC was found to behave in a much more flexible manner and resited cracking by subjecting a greater length of pipe to the dip displacement. Through the analysis it was determined that the material of the pipe and also the joints and segment lengths contribute heavily towards its performance against pipe dipping, thus these factors should be explored further to complement and enhance these findings.
- An investigation into performance of different trench materials also yielded some useful insight. Firstly, it was found that for pipes in liquefaction susceptible areas, there was a tendency for these pipes to suffer a loss of grade (i.e. fail the WLG criterion) when their trench material consisted of locally excavated sands/soils. It was speculated that due to liquefaction, some pipes experience a 'floating effect' causing their elevation exceed the upstream manhole elevation. This was opposed by results which showed more failures of the Backwash Potential criterion for AP20/AP40 mixtures. Again, it was speculated that this result was potentially due to manhole movement in addition to the buoyancy of pipes due to liquefaction. It is recommended that further investigation in the effects of manhole movement are conducted to better understand these findings.
- Due to lack of sufficient data representing pipe diameters, it was sensible not to pursue this potential factor as no confident conclusions could be obtained by statistical analysis. The justification to neglect this factor was based on the knowledge that the majority of the wastewater system contains diameters of very similar dimensions (150 to 225 mm).

6. ACKNOWLEDGMENTS

We would like to acknowledge the contributions made by SCIRT, in particular, David Heiler and Martin Dasler to the direction of the project and Irmana Sampedro for her efforts in collating data. Extra acknowledgement and thanks is given to Matthew Hughes of the University of Canterbury for his contributions.

7. REFERENCES

Cave, S. (2013). Investigation into the Effectiveness of Pipe Backfill Methods on Pipe Resilience against Dipping. SCIRT, Christchurch. Unpublished report.

Christchurch City Council. (2011). Infrastructure Design Standard Part 6 – Wastewater Drainage. Christchurch, Canterbury, New Zealand.

Cubrinovski, M., Hughes, M., Bradley, B., McCahon, I., and Y. McDonald (2011). Liquefaction Impacts on Pipe Networks. *Civil & Natural Resources Engineering Research Report 2011*. University of Canterbury.

Cubrinovski, M., & Taylor, M. (2011). Liquefaction map of Christchurch based on drive-through reconnaissance after the 22 February 2011 Earthquake. Christchurch, Canterbury, New Zealand: University of Canterbury.

Henderson, B. and McDonald, Y. (2013). Infrastructure Recovery Technical Standards and Guidelines, 4.3. Christchurch City Council, Christchurch, New Zealand.

Menefy, B., & Scally, D. (2013). Analysis and design of manholes in liquefiable soils. Christchurch, Canterbury, New Zealand: University of Canterbury.

Yukich, K. (2013). Profilometer Designers Guideline, SCIRT, Christchurch, New Zealand. Unpublished Report.

Appendix B: Liquefaction Induced Damage to Roads in the 2010-2011 Christchurch Earthquakes

Liquefaction Induced Damage to Roads in the 2010-2011 Christchurch Earthquakes

C. Barber and J. Meys

Final Year Projects, 2014
Dept. of Civil and Natural Resources Engineering
University of Canterbury
Project supervisor(s): M. Cubrinovski and M. Hughes

Keywords: *Roads, liquefaction, Christchurch earthquakes, geotechnical analysis, GIS.*

ABSTRACT

The 2010-2011 Canterbury earthquake sequence caused severe damage to many roads in Christchurch. Multiple sets of data were compared to investigate the causes, mechanisms and extent of road damage as well as the validity of the widespread assumption that liquefaction was the overwhelming cause of road damage. The most important data sets related to liquefaction observations, Peak Ground Velocity (PGA), road damage and road surface type. Statistical, geospatial and technical analysis of the data returned key findings. Road surface type was not a significant factor in how well roads performed, with the exception of 'single coat seal' which performed slightly better than other common surfaces. Liquefaction appeared to be insignificant at PGAs below 0.3g with correspondingly low road damage. After comparison of data from the majority of the Christchurch road network, liquefaction does indeed appear to have a strong, but not complete influence on how much damage the roads sustained. All conclusions are only indications of overall trends due to the highly variable nature of road damage and liquefaction.

1. INTRODUCTION

After the 2010 and 2011 Christchurch earthquake sequence, a large proportion of the city's road network was damaged. The majority of the damage was caused by the 22 February 2011 magnitude 6.2 earthquake, which caused widespread liquefaction and liquefaction-induced lateral spreading throughout the city. Some minor damage also resulted from the 4 September 2010 magnitude 7.1 earthquake, but the road damage from this event was far less significant. Although the September earthquake was of higher magnitude, the severity and extent of liquefaction was much higher in the February event due to its proximity to the city. In particular, the February earthquake produced large amplitude ground movements which were capable of inducing liquefaction over large areas of the city.

This project analyses a large variety of existing data from many different sources in order to explain and discuss how Christchurch's road network performed during the aforementioned earthquakes and in particular the 22 February 2011 earthquake.

1.1. Key Objectives

Specific questions that were addressed included:

- Which road surface constructions performed the best?
- How did earthquake peak ground acceleration (PGA) affect the roads?
- Was liquefaction the main cause of damage?
- How reliable was the available data?
- What level of PGA was required to cause a given level of road damage?

It is hoped that this research will go a long way with aiding engineers in predicting potential damage to Christchurch roads in future earthquakes. Additional research could be undertaken in this field. With further analysis, the data from Christchurch could be used to develop models for road damage prediction in other cities in New Zealand and globally.

This report will introduce the reader to the large variety of earthquake damage data that became available after the earthquakes thanks to the efforts of the Christchurch City Council (CCC), local engineering establishments and University of Canterbury researchers.

These data sets include:

- liquefaction severity map
- liquefaction resistance index (LRI) map
- road damage data
- road surface construction
- peak ground acceleration (PGA) contours
- peak ground velocity (PGV) contours.

Each of these data sets will be introduced in detail in the subsequent sections.

1.2. Effects of the 2010-2011 Earthquakes on Christchurch Roads

The September 2010 earthquake caused some damage to a small number of roads. The exact extent of this damage was never clearly documented and was overshadowed by the February 2011 event.

Following the February 2011 earthquake, the Christchurch road network was critically damaged, along with a large portion of the city itself. It appeared that the majority of the damage was due to underlying soils liquefying. The liquefied soil produced sand and silt ejecta, temporary flooding and significant and widespread deformation of road surfaces. Some of the flooding and damage was also caused by broken pipes buried beneath the road.

1.3. Emergency Response and Earthquake Recovery

In a number of cases, damage was bad enough to prevent road use altogether. Additionally, some key bridges were closed due to safety concerns and in isolated cases in the Port Hills area, rock falls caused road closures.

The inaccessibility of some roads hindered emergency services which prioritised functionality restoration of lifeline roads. Extensive emergency works were carried out to regain drivability on some roads, particularly those that were isolating neighbourhoods or blocking arterial routes. A concerted effort was made by the community to clear the large quantities of liquefaction ejecta from the roads.

Eastern Christchurch residential areas and much of the Christchurch Central Business District (CBD) was cordoned off for safety reasons and established as the 'red zone'. This put significantly more pressure on arterial routes around the red zone resulting in ongoing traffic congestion.

1.4. Medium to Long Term Issues with the Road Network

Following the initial disaster response, the road network was in an extremely poor condition. Many roads were deformed to the extent that the resulting ride was extremely uncomfortable. Widespread problems such as horizontal cracking, vertical cracking, ponding, broken kerb and channel, cracked footpath and potholes compromised road usability and safety. Additionally, without a quick temporary response, many small defects would rapidly deteriorate with traffic use.

Christchurch City Council (CCC) conducted a survey of the road network, summarising the steps taken in a report (McNeill and English, 2014). This report has not been formally released but appears to conclude that the road network would need approximately $375 million in repairs. This is over 12% of the estimated $3 billion the government expects to be needed for infrastructure repair and replacement following the earthquake (Parker and Steenkamp, 2012).

After initial stabilisation works such as filling potholes and injecting rubber into cracks to prevent further deterioration, road repair crews continue to fully rehabilitate important sections of road, gradually restoring the road network.

2. AVAILABLE DATA

After the February 2011 earthquake, a geotechnical reconnaissance of Christchurch was carried out by University of Canterbury academics alongside colleges from other universities. Their findings were summarised in the paper titled Geotechnical Aspects of the 22 February 2011 Earthquake. As part of this paper, a map of observed liquefaction was developed. This map, shown in Figure 1, was produced by categorising liquefaction based on observations made during a drive through of affected areas. The moderate to severe liquefaction category referred to areas covered by sand ejecta, large ground cracks and fissures. Low to moderate liquefaction is defined as some ejecta with noticeable deformation. Trace liquefaction denotes areas of liquefaction limited in severity and extent. No surface manifestation of liquefaction was evident in areas labelled as no liquefaction (Cubrinovski et al., 2011).

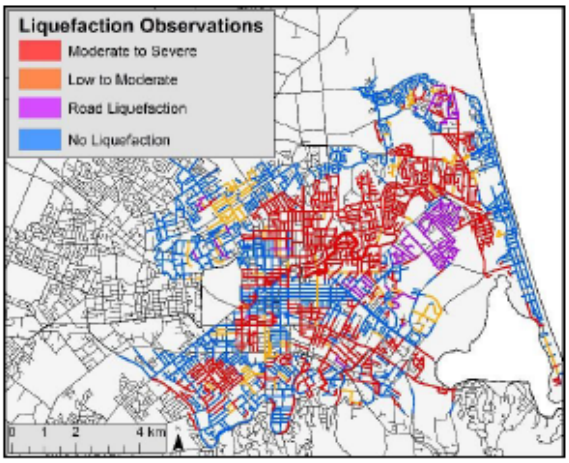

Figure 1. Map of observed liquefaction made during a drive through after the 22 February 2011 earthquake (Cubrinovski et al., 2011)

An important tool that was used extensively for this project was the PGA contour map developed by Bradley and Hughes (2012). During each of the earthquake events in 2010 and 2011, accelerations and hence PGAs were recorded at a number of strong motion stations located throughout Christchurch. By interpolating between each motion station using a probabilistic model, the PGA at any location within the city and surrounding area was

predicted. These predictions are conditional on the specific value of PGA recorded at each strong motion station. As such, the predicted PGA values were termed as 'conditional' (Bradley and Hughes 2012). Figure 2 shows the PGA contour map derived from the observed ground motions during the February 2011 earthquake. The same method was applied in creating the PGV map which is not shown because it offers a similar evaluation measure as the PGA map.

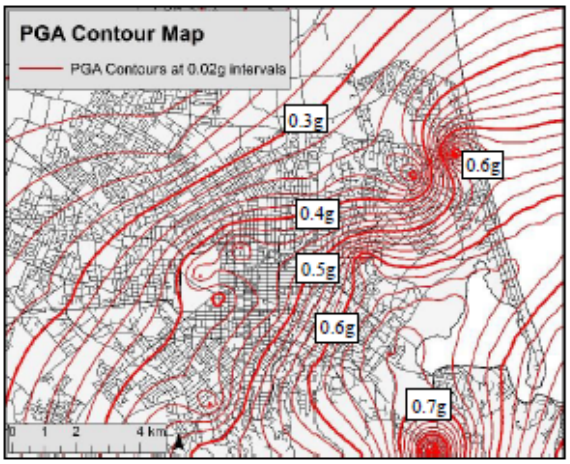

Figure 2. Conditional PGA contour map of the 22 February 2011 earthquake (Bradley and Hughes 2012)

3. METHODOLOGY

Analysing the effects of the February 2011 earthquake on the road network required detailed comparisons of a number of important data sets. The majority of the investigation was the acquisition, validation and manipulation of relevant data sets so that they could be justifiably compared to one another.

3.1. CCC Road Damage Rating

One key aspect of this project was understanding how the CCC developed its road damage rating. Several meetings were had with Steve McNeill and Geoff English who were the CCC engineers responsible for developing the road damage rating. By discussing the process they went through following the earthquake, it was possible to gain an understanding of how useful this damage rating would be in analysing the damage to the road network.

Estimates for the road network rebuild were made after the 4 September 2010 earthquake. Initial data capture of road damage focussed on damage to the carriageway, kerb and channel, and footpaths. This data was collected by teams of staff from the council, NZTA and transport consultancies. All information was uploaded into RAMM (Road Asset and Maintenance Management software). Repair cost estimates were developed for a number of sites.

Following the February 2011 earthquake and the realisation of the widespread road damage across the city, the CCC commissioned immediate emergency repairs and road closures. An initial estimate of the total repair cost of the network was made based on the quantities of silt removal and other sources of damage observations. However, this was only a preliminary estimate. Methodology for improved assessment of road damage was later developed. Also, standard fault types were developed based on the most commonly observed types of road damage across the city. Types of damage fell into one of four categories; pavement, drainage, footpath and kerb and channel. Table 1 shows two examples of standard fault types. Unit cost rates of repair were assigned to each type of damage. The costs were calculated based on standard pre-earthquake contractor rates then appreciated to reflect the then depressed road repair market.

Ten teams of similarly skilled people to those used in the September 2010 data collection were trained in the use of Pocket RAMM, a mobile, handheld, geo-tagging device. This enabled road damage survey teams to easily and accurately geotag individual damage points across the city. Location and severity of damage were recorded based on observations made from a vehicle. Localised data collection was performed following the June and December 2011 earthquakes. One team was used to audit the work of the other teams. Table 1 shows an example of the types of inputs being made into Pocket RAMM. In total, there were 40,475 data points logged by the ten teams over a period of 12 weeks.

Table 1. Example of Pocket RAMM inputs

Asset Type	Fault	Start (m)	End (m)	Length (m)	Width	Side (m)
EQ Pave Failures	Crack under 20mm – Rubber	109	110	1	1.5mm	Right
EQ K&C Repairs	Flat CHNL – Broken <10m	349	350	1	1m	Left

From a geographic information systems (GIS) perspective, roads in Christchurch were broken into sections that generally varied in length from around 50 to 500 meters with an average length of 230 meters. Roads were generally split into segments at intersections, with care being taken to adjust the section length to avoid overlapping at these locations. For example, Ferry Road, which is over 6km in length, was split into 30 smaller sections.

Discrete damage points obtained from Pocket RAMM were imported into Excel and multiplied by their respective repair unit rate, keeping pavement, kerb and channel and carriageway separate (drainage was

addressed in a different manner that will not be discussed in this paper). Asset replacement costs were calculated based on historical data. The cost to repair individual damage points lying on the same road segment were summed to find the total cost to repair each segment. The ratio of repair cost to replacement cost for each segment was then calculated. This ratio, expressed as a percentage, defined the damage rating for each segment. This can be seen in Table 2 which also includes a qualitative description of the damage corresponding to each damage rating.

Table 2. Road damage rating and corresponding percentage of repair cost

Percentage of Road Damage	Damage Rating
0%	No Damage, 0
0-1%	Minimal, 1
1-10%	Minor, 2
10-50%	Moderate, 3
50-75%	Major, 4
>75%	Severe, 5

Damage ratings were kept separate between the carriageway, footpath and kerb and channel, depending on where the recorded damage was located. In order to give an individual road segment an overall street damage rating, a weighted average of these three categories was calculated as follows.

$$DR_{street}=0.5*DR_{kerb\&channel}+0.4*DR_{carriageway}+0.1*DR_{footpath}$$

The damage rating coefficients shown above reflect the overall contribution of individual street components to the cost and reparability of the street as a whole. Kerb and channel was given the highest weighting as damage to this asset can cause poor flow of water and flooding. Also, it was also more complex to make kerb and channel repairs compared to the carriageway. Footpaths were given the smallest factor as they could be easily repaired or replaced compared to the two other assets. Although the combined street rating is somewhat based on the functionality of the street, it still very much remains an economic representation of damage because repair costs increase with increasing complexity.

Should road damage exceed 75% of its renewal cost, the CCC made the decision to renew the entire road. This decision reflected the small amount of additional cost that would be required to replace the road instead of completing repairs. For the purposes of this project, it was decided to merge the no damage and minimal damage ratings. This was because the difference between 0% and 1% damage was considered to be too small to justify a standalone category. The street damage map is shown in Figure 3.

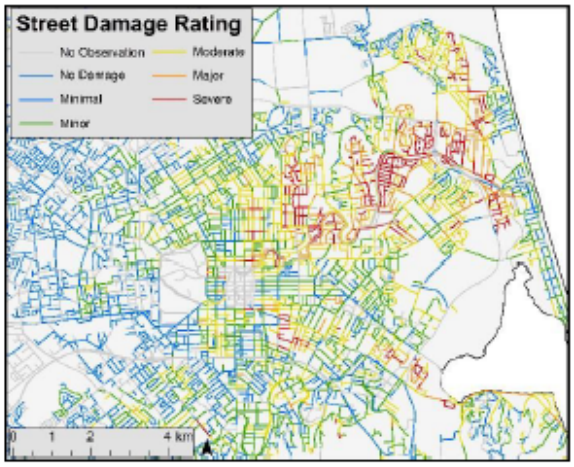

Figure 3. Street damage rating showing combined colour of no damage and minimal ratings

3.2. Road Surface Data

From the RAMM database, which contains a large amount of useful road data for contractors, it was possible to extract the maintenance history of the Christchurch road network. This 18000 entry dataset had columns that indicated the date each road surface was built, surface type, and chainage values for the start and end of the surface.

To get this data into a format compatible with any other data set, heavy procedural manipulation was necessary. This was out of the range of capabilities of Excel so database software Microsoft Access was used.

Firstly, the road surfaces were overlaid on top of one another in chronological order so the old surfaces were overwritten. This was necessary to replace partial or complete road surfaces that had since been renewed, thereby giving a final output representative of the September 2010 road network.

Secondly, the resulting patchwork of current road surfaces was cross referenced with different road sections that included damage rating data. For each road section, the road surface that was most prevalent was chosen to be representative. This process introduced some error because there were many cases where one road section included other surface types. The final road surface map is shown in Figure 4.

The validity of only taking the dominant surface type for each road section was checked. An analysis of how much the dominant surface covered each section was undertaken. From this it was possible to determine that on average, 86% of each road section was the dominant surface and therefore correctly represented. The road data was only used to give an indication of possible trends and for this purpose, the inaccuracy introduced was thought to be tolerable.

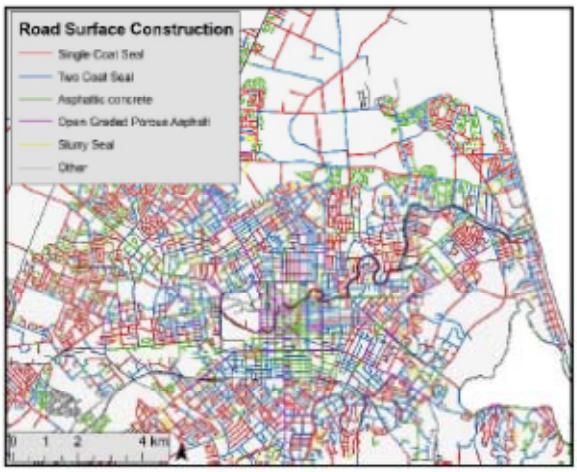

Figure 4. Road surface composition of the Christchurch road network. Other roads are those with less than 300 individual data entries

3.3. Obtaining Data and Data Sources

The majority of the required shape files were from Matthew Hughes who sourced them through his well-established contact network and involvement with similar projects. These data sets included the original CCC road network spatial layout, liquefaction observations, LRI, LiDAR, PGA and PGV. Road surface data was obtained from RAMM. The spreadsheet containing the original footpath, carriageway and kerb and channel damage ratings was obtained from Steve McNeill and Geoff English as explained in Section 3.1.

3.4. Manipulating and Overlaying GIS Data Sets

GIS software, in particular ArcMap 10.2, was used for this project. This software takes shape files and displays them as a geospatial map. All of the map figures in this report are examples of the types of displays ArcMap is capable of producing. Using ArcMap, it was possible to overlay and relate the many available spatial datasets.

A shape file is a type of database file that stores a geographic co-ordinate with each individual data point. This geographical co-ordinate can then be expressed as a point, a line, a polygon or a raster within ArcMap. Points and lines are self-explanatory, however, polygons and rasters require some additional explanation. Polygons are data representations that cover a two dimensional area on the map. An example of a polygon data set is the liquefaction observation map displayed in Figure 1. Raster shape files represent a grid or matrix of data. The PGA data set represented in Figure 2 is an example of this. Every five square metres of the Christchurch area was assigned an individual conditional PGA value based on the work completed by Bradley and Hughes.

To display the data correctly, it must first have an appropriate coordinate system attached to it. This project used the NZGD 2000 New Zealand Transverse Mercator coordinate system which is a typical Mercator system used in New Zealand.

The first challenge in being able to overlay the different shape files available was applying the correct coordinate system. Some files were set in different systems and needed to be manipulated in order to be used. By using the "Projections and Transformations" tools in ArcMap is was possible to streamline all of the different coordinate systems.

Data sets were compared by spatially overlaying them with one another. This was made possible using the "Overlay" tools within ArcMap. Lines were converted into points for this process as any line that was not completely enveloped by a polygon or raster was not considered to be intersecting. Each road section was converted into a point located at the centroid of the road. Straight roads would have the point located in the middle of the section while curved roads would have it located within the vertex of the corner. This method of conversion meant some data that may have been partially overlapping another data set was lost. However, the amount of data loss was considered to be negligible and any data that was lost had only a small proportion of overlap. Minimal data was lost when overlaying the road data with PGA and PGV as both of these data sets encompassed the entire city.

3.5. Comparing Data Sets and Identifying Trends

All data comparison and statistical analysis was performed in Excel. Having overlaid all data sets, a single master spreadsheet was exported from ArcMap. Each row in this spreadsheet represented a single road segment as well as the associated PGA, PGV, observed liquefaction, damage ratings, LRI and road surface construction. Not every road intersected with every data set so there were many instances where no data existed.

Individual data sets were isolated easily by simply sorting by the required variable and copying that section out of the master spread sheet for analysis. This process was followed, along with the use of built in Excel functions, to produce the tables, figures and results shown in the proceeding section.

4. RESULTS, ANALYSIS AND DISCUSSION

4.1. Performance of the Christchurch Road Network

An analysis of the street damage rating, shown as a map in Figure 3, can be seen in Figure 5. This figure shows that only a small proportion of the road network was severely damaged. 48% of the roads in Christchurch suffered no damage to minor damage (0-10% damage). 35% of the road network was not surveyed by the CCC

after the February 2011 earthquake. This reflects the concentration of road damage within the urban reaches of the city.

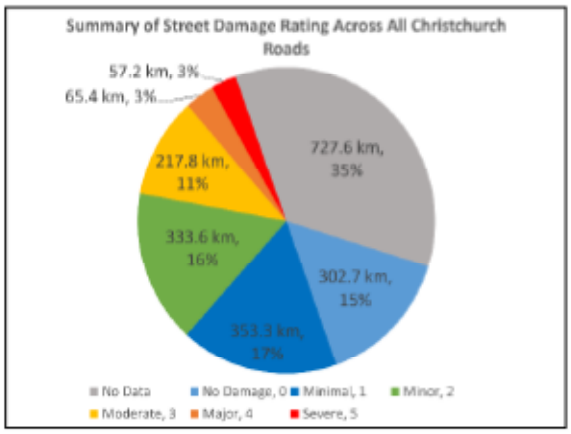

Figure 5. Summary of street damage rating across the Christchurch road network after the 22 February 2011 earthquake (total 2058 km)

4.2. Comparison of PGA with Road Damage and Liquefaction Observations

In Figure 6, percentage street damage was compared to PGA, and liquefaction observations were separated into categories. The data was highly variable and for easier trend identification, a 30 point centred moving average was overlaid for each liquefaction observation category. Average street damage percentage for multiple PGA ranges is displayed in Table 3.

Box and whisker sections within Figure 6 indicate the spread of road damage data when classified by observed liquefaction type. The box indicates the lower and upper quartiles of road damage and the whiskers represent the 10th and 90th percentiles.

Table 3. Summary Road Damage Compared to PGA

PGA Category	Average Road Damage
< 0.2g	0.3%
0.2-0.3g	1.4%
0.3-0.4g	24.3%
0.4-0.5g	20.4%
0.5-0.6g	20.4%
0.6-0.7g	14.4%
Average	16.3%

In Figure 6, street damage showed a reasonably clear correlation with observed liquefaction. The 30 point centred moving average for the moderate to severe liquefaction was considerably higher than that of the no liquefaction observation. The low to moderate liquefaction fell between the two extreme categories as expected. The median damage for all PGA values was approximately 0.3% for no liquefaction, 6.3% for low to moderate liquefaction and 40% for moderate to severe liquefaction.

The strong correlation between liquefaction and road damage was expected because it backs up field observations that liquefaction was the primary cause of road damage.

The relationship between PGA and road damage was not immediately clear. Black dotted lines on Figure 6 show apparent threshold values of PGA. The first threshold

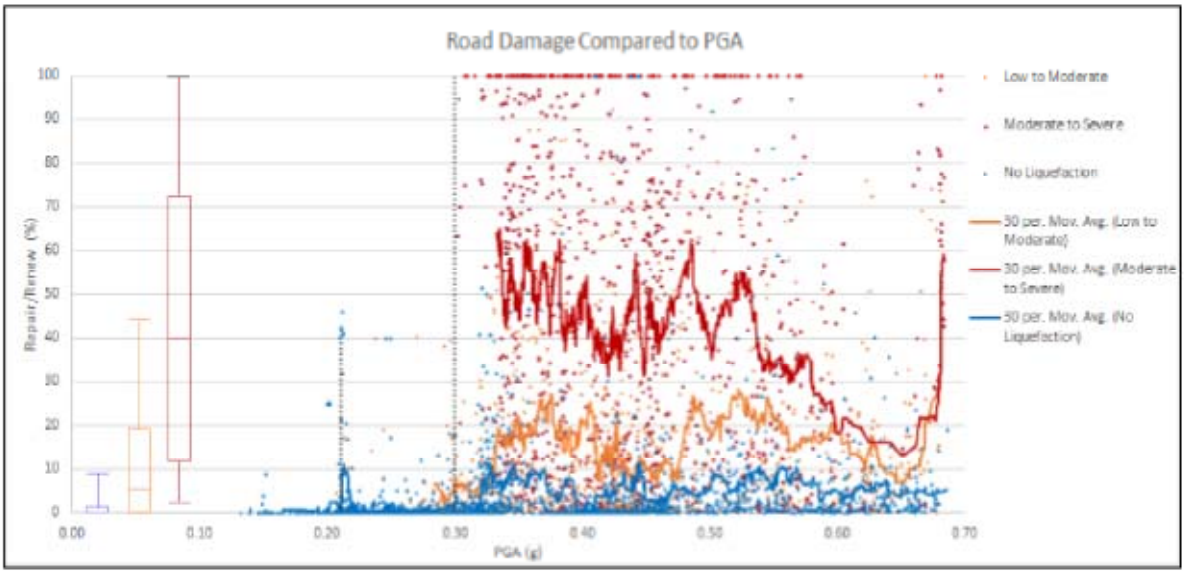

Figure 6. Comparison of percentage of street damage to PGA, isolating liquefaction observation categories.

was at a PGA of approximately 0.2g. Below 0.2g, road damage did not exceed 10% and averaged just 0.3%.

This showed roads in Christchurch that experienced less than 0.2g remained virtually undamaged. The second threshold value was approximately 0.3g. Between 0.2g and 0.3g, the damage to roads averaged 1.4%. There were a small number of cases in which road damage reached approximately 40% but 50% was not exceeded. This means that isolated cases of moderate road damage begin to appear at PGA values of between 0.2g and 0.3g. PGAs that exceed 0.3g immediately show a pronounced difference. In fact, PGA values between 0.3g and 0.4g have the highest average damage rating of 24.3%. There are numerous cases where damage has reached 100%, indicating the need for complete renewal of a road section.

Road damage becomes significantly worse when the observed threshold value of 0.3g is exceeded. The most likely explanation for this effect is that typical Christchurch soils require a PGA of 0.3 or higher to cause significant liquefaction. This is supported by the liquefaction observation data in Figure 6 which had no records of moderate to severe liquefaction below a PGA of 0.3g.

Interestingly, progressing beyond a PGA of 0.3g, road damage did not continue to worsen. Instead it appeared to fluctuate evenly around approximately the same value. The only significant deviation from this was the pronounced drop in road damage between accelerations of 0.55g and 0.65g in areas that moderate to severe liquefaction were observed.

The high number of data points was necessary to overcome the large discrepancies caused by localised ground and road features. However, systematic errors across the entire data set remain a concern. One possible source of systematic error is that PGA values are specific to certain regions. It is entirely possible that a particular ground condition or feature falls exclusively into a specific range of PGA values causing the misguided appearance of the influence PGA has on road damage or liquefaction. A possible example of this is within the Port Hills and Heathcote Valley areas where the PGA values were high but the ground conditions had a strong resistance to liquefaction. This could possibly account for the unexpected drop in road damage at PGA values between 0.55g and 0.65g.

Although PGA was used for comparison, PGV and shaking duration are also major contributors to liquefaction induced physical damage. PGA and PGV were investigated and as expected, showed a very strong correlation with one another as the both data sets were derived from the same acceleration time history. This means that attempting to find the relationships between PGV and liquefaction or road damage would return similar results to that of PGA. Individually comparing PGV to the available data was therefore deemed unnecessary.

It is worth noting that the results are inconsistent if small data sets are used or small areas are inspected. This shows that localised features and highly variable ground conditions played an important role in determining how much damage any particular road section sustained.

4.3. Performance of Road Surfaces

Figure 7 shows the most predominant carriageway surface types compared to sustained damage. To enable easier identification of trends, the data has been normalised, ensuring the damage category adds to 100% across every road surface type. This removes distorting effects such as the existence of more data points in the minimal damage category compared to the severe category. Figure 7 therefore shows which road surface types are most common, indicated by the larger datasets.

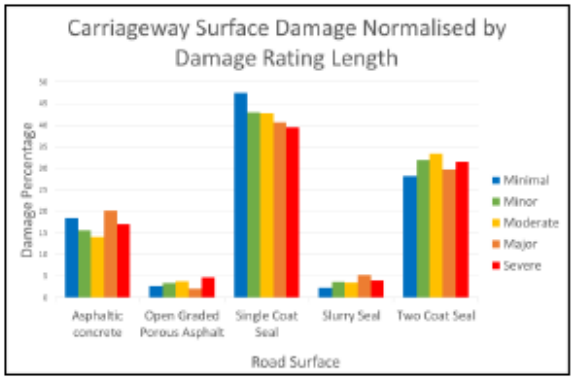

Figure 7. Performance of predominant carriageway surfaces.

Less common road surface types such as concrete and open graded emulsion were omitted because they were seen to have an insufficient amount of data for a meaningful analysis.

Figure 7 shows the most apparent trend is most road surfaces show an even distribution of damage severity. This suggests that road surface type did not have a significant effect on how much a road would cost to repair after the earthquakes. This is backed up by the work of Pidwerbesky and Waters (2011) who found that, "inspection showed most pavements had performed well and that the damage to the pavements was caused by failures beneath the pavement".

Single coat seal was the only road surface that showed a clear trend. It exhibited more cases of minimal damage compared to severe damage with the minor, moderate and major categories conforming to this trend. Single coat seal is among the thinnest and cheapest road surfaces. It is also one of the most common.

It is therefore possible that a thin and flexible road surface performs better in earthquakes. Another conclusion could be that repairing the common and simple single coat seal is simply cheaper than other surfaces when compared to the capital value of the road. Most importantly, this supports the findings from the Christchurch Pavement Resilience Investigation. Pidwerbesky and Waters (2011) state that "the most resilient pavements in seismic events, considering factors such as level of service after the events, survivability of the pavement and economics of repair, are thin-surfaced unbound granular and foamed bitumen stabilised pavements".

It is worth noting that in the data available there was no mention of the subgrade used. This could have had more of an effect on the performance of the road than the road surface which is typically much thinner.

Possible error could have been introduced if parts of Christchurch that were significantly affected by the earthquake had a higher tendency toward a particular road type. From Figure 4, it appears that there is a good spread of road types across the city, however, numerically verifying this is time consuming.

5. CONCLUSION

Primary data sets that were compared were liquefaction observations, PGA, road surface type and road damage. Road damage was the percentage of the repair cost in relation to the replacement cost of the road section.

The validity of each data set was investigated and it was determined that, although the data showed high local variance, the quantity of data allowed meaningful conclusions to be drawn based upon averages and overall trends.

Road surface type was found to have no noticeable effect on the damage sustained by liquefaction. The exception to this is the single coat seal road surface which appeared to sustain lower damage than other common road surfaces in Christchurch. This is supported by Waters and Pidwerbesky who showed similar findings when the performance of road surfaces was investigated experimentally and by observation.

The relationship between road damage and observed liquefaction was strong overall. Areas with no observed liquefaction had overall road damage of approximately 0.3%, low to moderate observed liquefaction indicated overall damage of 6% and areas showing moderate to severe liquefaction had overall road damage of roughly 40%.

When the road damage was compared to PGA it was found that a PGA below 0.3g appeared to have little effect on the roads, shown by an average of less than 2% road damage. Road damage became significantly more severe at a PGA of approximately 0.3g and remained approximately constant at roughly 20% up to the highest PGA values of 0.7g. It is most likely that the reason for this phenomenon is Christchurch soils require approximately 0.3g or higher to trigger damaging liquefaction.

6. ACKNOWLEDGEMENTS

The authors would like to express a special thanks to Misko Cubrinovski and Matthew Hughes. Misko's technical expertise and direction were crucial in the development of the project. Matthew provided much of the important data through his extensive professional network and instructed the authors in the workings of GIS software. The authors would like to thank them for giving up their time to guide and mentor the authors through their first significant research project. Their patience and understanding was much appreciated.

This project would not have been possible without the help of Steve McNeill and Geoff English giving up their time to discuss how they created the original damage rating data and spreadsheet. It was a pleasure to have collaborated with such esteemed engineers.

Usage of a road surface data would not have been possible without the help of Dominic Lo who assisted the authors in manipulating the road surface construction data so it was able to be merged with other data sets.

7. REFERENCES

Cubrinovski M., Bradley B., Wotherspoon L., Green R., Bray J., Wood C., Pender M., Allen J., Bradshaw A., Rix G., Taylor M., Robinson K., Henderson D., Giorgini S., Ma K., Winkley A., Zupan J., O'Rourke T., DePascale G and Wells D. (2011), Geotechnical aspects of the 22 February 2011 Christchurch earthquake, *Bulletin of the New Zealand Society for Earthquake Engineering*, 44(4), 205 - 226.

Bradley B. and Hughes M. (2012), Conditional peak ground accelerations in the Canterbury earthquakes for conventional liquefaction assessment, technical report prepared for the Department of Building and Housing.

McNeill S. and English G. (2014), internal and unpublished documentation and discussion.

Waters J. and Pidwerbesky B. (2011), Christchurch pavement resilience investigation, technical report prepared for the Stronger Canterbury Infrastructure Rebuild Team.

Parker M. and Steenkamp D. (2012), The economic impact of the Canterbury earthquakes, *Bulletin*, Reserve Bank of New Zealand, 75(3), 13 - 25.